Resilient Vertical Forest Renovation of Reinforced Concrete Structures in Seismic Prone Areas
(H.F.R.I. Project Number 015376)

Designs and photos of detailing and instrumentation of constructed as-built 3d structure

Deliverable D2.1 Work package 1

Funding source

"Hellenic Foundation for Research & Innovation (H.F.R.I.)
Greece 2.0
Basic Research Financing Action"

Host Organization

Democritus University of Thrace (DUTH)

Collaborating Organizations
Aristotle University of Thessaloniki (AUTH)

November 2024

Funded by the European Union
NextGenerationEU

The research project is implemented in the framework of H.F.R.I call "Basic research Financing (Horizontal support of all Sciences)" under the National Recovery and Resilience Plan "Greece 2.0" funded by the European Union – NextGenerationEU (H.F.R.I. Project Number: 015376)

Version	Date	Comments-Modifications
1	November 2024	Final Version
2		

Suggested citation:

Rousakis T., Voutetaki M., Kellis S., Zapris A., Lappa M., Xynopoulos I., Sapidis G., Papadopoulos N., Karampini M., Mallinis G., Stefanidou M., Theodoridou I., 2024. *Designs and photos of detailing and instrumentation of constructed as-built 3d structure*. Greenergy-Resilient Vertical Forest Renovation of Reinforced Concrete Structures in Seismic Prone Areas (H.F.R.I. Project Number 015376). Deliverable D2.1 Democritus University of Thrace, Xanthi.

Project Title	Resilient Vertical Forest Renovation of Reinforced Concrete Structures in Seismic Prone Areas
Acronym	GREENERGY
HFRI Project Number	015376
Call identifier	Basic Research Financing (Horizontal support for all Sciences), National Recovery and Resilience Plan (Greece 2.0) / Sub-action 2. Funding Projects in Leading-Edge Sectors – RRFQ: Basic Research Financing (Horizontal support for all Sciences)
Thematic area	ThA1. Physical Sciences, Engineering Sciences and Technology, Environment and Energy
Thematic Field	1.16 Smart Cities
Host Organization	Democritus University of Thrace
Collaborating Institutions	Aristotle University of Thessaloniki
Project starting date	13/3/2024
Project Principal Investigator	**Dr. Theodoros Rousakis**
Affiliation	**Democritus University of Thrace / Department of Civil Engineering**
Email	**trousak@civil.duth.gr**
Telephone	25410 79645, 461 / 6977421569
Deliverable number and title	*D2.1 Designs and photos of detailing and instrumentation of constructed as-built 3d structure*
Related work package	**WP2** – Experimental dynamic assessment of physical model structure towards holistic renovation
Authors	Theodoros Rousakis, Maristella Voutetaki, Stefanos Kellis, Adamantis Zapris, Martha Lappa, Ioannis Xynopoulos, Georgios Sapidis, Nikolaos Papadopoulos, Martha Karampini (DUTh) Georgios Mallinis,Maria Stefanidou,Ifigeneia Theodoridou (AUTh)

Τίτλος Έργου	Ανθεκτική Αντισεισμική Ανακαίνιση Κατασκευών από Ωπλισμένο Σκυρόδεμα σε Κάθετο Δάσος
Ακρωνύμιο	GREENERGY
Αριθμός Έργου ΕΛΙΔΕΚ	015376
Δράση	Χρηματοδότηση Βασικής Έρευνας (Οριζόντια υποστήριξη όλων των Επιστημών), Εθνικό Σχέδιο Ανάκαμψης και Ανθεκτικότητας (Ελλάδα 2.0)
Θεματική Περιοχή	ΘΠ1. Φυσικές Επιστήμες, Επιστήμες Μηχανικού και Τεχνολογίας, Περιβάλλον και Ενέργεια
Θεματικό Πεδίο	1.16 Έξυπνες Πόλεις
Φορέας Υποδοχής	Δημοκρίτειο Πανεπιστήμιο Θράκης
Συνεργαζόμενος Φορέας	Αριστοτέλειο Πανεπιστήμιο Θεσσαλονίκης
Ημερομηνία έναρξης Έργου	13/3/2024
Επιστημονικά Υπεύθυνος Έργου	**Δρ. Θεόδωρος Ρουσάκης**
Ίδρυμα / Τμήμα	**Δημοκρίτειο Πανεπιστήμιο Θράκης / Πολιτικών Μηχανικών**
Email	**trousak@civil.duth.gr**
Τηλέφωνα	25410 79645, 461 / 6977421569
Αριθμός και Τίτλος Παραδοτέου	***Π2.1*** *Σχέδια και Φωτογραφίες λεπτομερειών και ενοργάνωσης της υφιστάμενης κατασκευής*
Σχετική Ενότητα Εργασίας	**ΕΕ2** – Πειραματική δυναμική αποτίμηση του φυσικού προσομοιώματος της κατασκευής προς την ολιστική ανακαίνιση
Συγγραφείς	Θεόδωρος Ρουσάκης, Μαριστέλλα Βουτετάκη, Στέφανος Κέλλης, Αδαμάνυης Ζάπρης, Μάρθα Λάππα, Ιωάννης Ξυνόπουλος, Γεώργιος Σαπίδης, Νικόλαος Παπαδόπουλος, Μάρθα Καραμπίνη (ΔΠΘ) Γιώργος Μαλλίνης, Μαρία Στεφανίδου, Ιφιγένεια Θεοδωρίδου (ΑΠΘ)

ACKNOWLEDGEMENTS

This project is carried out within the framework of the National Recovery and Resilience Plan Greece 2.0, funded by the European Union – NextGenerationEU (Implementation body: HFRI).

TABLE OF CONTENTS

LIST OF TABLES

LIST OF FIGURES

LIST OF ACRONYMS

VF	Vertical Forest
RC	Reinforced Concrete
PZT	Piezoelectric sensors or piezoelectric transducers
3D	3 Dimensions
etc	et cetera
D21	Deliverable 21
e.g.	for example
PFJ	Polymer Flexible Joints
PUFJ	Polyurethane Flexible Joints
PM - soft	Soft Polymeric Materials
PT- stiff	Stiff Polymeric Materials
PS – middle stiff	Middle Stiff Polymeric Materials
CFRP	Carbon Fiber-Reinforced Polymers
PTMS	Post – Tensioned Metal Straps
WiAMS	Wireless impedance/Admittance Monitoring System
SHM	Structural Health Monitoring
CO2	Carbon dioxide
EMI	Electromechanical Impedance
DUTH	Democritus University of Thrace
NTUA	National Technical University of Athens
PID controller	Proportional–integral–derivative controller
SAs	Strain guages
USA	United States
AUTH	Aristotle University of Thessaloniki

ABSTRACT

GREENERGY envisions forest diffusion to alleviate extreme weather conditions impacts in coastal seismic urban regions and to optimize inclusive people-centric social engagement towards habitant comfort and satisfaction, through high-density urban forestation starting from green- renovated buildings. Based on the poor state of the art in the field of renovation towards vertical forests and the great necessity for their urgent development, GREENERGY aims to really cope with detrimental climate change consequences and advance environmental resilience. In that aspect, the experimental quantification of the influence of critical parameters for green holistic renovation of common building to VF building with advanced structural, energy, forestry and habitant comfort performance is crucial. This deliverable concerns the designs and photos of detailing and instrumentation of constructed as-built 3d structure within the framework of workpackage of the experimental dynamic assessment of physical model structure towards holistic renovation. The one-bay, one-storey 3d-structure consists of a slab, four columns, four foundation beams and four brick infill walls. It is scaled down to the capacity of the seismic table of DUTh and refers to old generation design codes for reinforced concrete buildings, having sparse and inadequate steel stirrups and in general poor steel detailing. Further, low strength brick wall infills with low strength brick-joint mortar, cover the two opposite RC frames subjected to out of plane dynamic excitation. Finally, the two opposite RC frames subjected to in plane dynamic excitation include two partial brick wall infills of identical mechanical characteristics. The instrumentation of the structure involves advanced embedded a) innovative PZT sensors inside the concrete mass (columns, slab, and beams hidden in the slabs) as well as b) strain gauges, glued on the longitudinal bars of the four columns. Further, 3d accelerometers are attached on the slab, on the foundation beam and on the infill wall subjected to out of plane dynamic excitation. Finally, draw wire displacement meters are attached on the slab, on the foundation beams and along the diagonals of the partial infill walls subjected to in-plane dynamic excitations. The dynamic excitation of the seismic table will be based on the dynamic characteristics and severity of well-known disastrous Thessaloniki (Volvi) 1978 earthquake. With the as-built reinforced concrete brick infilled structure, GREENERGY aims to assess the dynamic performance of old type deficient structures with the next deliverable D23. GREENERGY envisions forest diffusion to alleviate extreme weather conditions impacts in coastal seismic urban regions and to optimize inclusive people-centric social engagement towards habitant comfort and satisfaction, through high-density urban forestation enabled with innovative and resilient renovations and structural health monitoring.

Keywords: experiment, seismic table, reinforced concrete, brick wall infills, seismic excitation, Vertical Forest, plant, resilience, renovation, structural, structural health monitoring, PZT

ΠΕΡΙΛΗΨΗ

Το έργο GREENERGY οραματίζεται τη διάχυση δασών για να μετριαστούν οι επιπτώσεις των ακραίων καιρικών συνθηκών σε παράκτιες σεισμογενείς αστικές περιοχές καθώς και να βελτιστοποιήσει τη συμπερίληψη της κοινωνικής συμμετοχής, επικεντρωμένης στους ανθρώπους. Στόχος του έργου είναι η άνεση και ικανοποίηση των κατοίκων, μέσω της αστικής δασοφύτευσης υψηλής πυκνότητας που ξεκινά από τα «πράσινα» ανακαινισμένα κτίρια. Το έργο GREENERGY λαμβάνει υπόψην τις υφιστάμενες ελλείψεις στην τεχνογνωσία στον τομέα των ανακαινίσεων που περιλαμβάνουν και κατασκευή κάθετων δασών (vertical forests) και την εξαιρετική ανάγκη για την επείγουσα ανάπτυξή της, στοχεύοντας να αντιμετωπίσει πραγματικά τις επιπτώσεις της κλιματικής αλλαγής και να προωθήσει την περιβαλλοντική ανθεκτικότητα. Σε αυτό το πλαίσιο, η πειραματική ποσοτικοποίηση της επίδρασης των κρίσιμων παραμέτρων για την πράσινη, ολιστική ανακαίνιση ενός συνήθους κτιρίου σε κτίριο με προσθήκη κάθετου δάσους (VF), με προηγμένη επιτελεστικότητα σε όρους δομικής αντοχής, ενέργειας, δασοκομίας και άνεσης των κατοίκων, είναι κρίσιμη. Αυτό το παραδοτέο αφορά τα σχέδια και τις φωτογραφίες της σκυροδετημένης κατασκευής και των λεπτομερειών όπλισης, των τοιχοποιιών πλήρωσης καθώς και της ενοργάνωσης του κατασκευασμένου, τρισδιάστατου μοντέλου. Απώτερος στόχος είναι η πειραματική δυναμική αξιολόγηση της κατασκευής προς την ολιστική ανακαίνιση. Η κατασκευή είναι μονόροφη με περιλαμβάνει πλάκα (με ενισχυμένες ζώνες κρυφοδοκών), τέσσερα υποστυλώματα και τέσσερις δοκούς θεμελίωσης καθώς και τέσσερις τοίχους πλήρωσης από τούβλα. Η κλίμακα της κατασκευής είναι προσαρμοσμένη στην ικανότητα της σεισμικής τράπεζας του ΔΠΘ (Δημοκρίτειο Πανεπιστήμιο Θράκης) και βασίζεται σε κανονισμούς σχεδιασμού παλαιάς γενιάς για κτίρια από οπλισμένο σκυρόδεμα, τα οποία έχουν αραιούς και ανεπαρκείς χαλύβδινους συνδετήρες και γενικότερα ανεπάρκειες στα υποστυλώματα. Επιπλέον, οι τοιχοπληρώσεις είναι χαμηλής αντοχής με κονίαμα αρμού χαμηλής αντοχής και καλύπτουν τα δύο απέναντι πλαίσια από οπλισμένο σκυρόδεμα που υφίστανται εκτός επιπέδου δυναμική διέγερση. Τέλος, τα δύο απέναντι πλαίσια από οπλισμένο σκυρόδεμα που υφίστανται δυναμική διέγερση εντός επιπέδου, περιλαμβάνουν δύο τοιχοπληρώσεις με τα ίδια μηχανικά χαρακτηριστικά που καλύπτουν μέρος του ανοίγματος. Η ενοργάνωση της κατασκευής περιλαμβάνει προηγμένα ενσωματωμένα α) καινοτόμα αισθητήρια PZT μέσα στη μάζα του σκυροδέματος (στα υποστυλώματα, στην πλάκα και στις κρυφοδοκούς) καθώς και β) παραμορφωσιόμετρα (strain gauges) κολλημένα στις διαμήκεις ράβδους των τεσσάρων υποστυλωμάτων. Επίσης, 3D επιταχυνσιόμετρα είναι τοποθετημένα στην πλάκα, στη δοκό θεμελίωσης και στους τοίχους πλήρωσης που υπόκεινται σε εκτός επιπέδου δυναμική διέγερση. Τέλος, μετρητές μετατοπίσεων με σύρμα (draw wire displacement meters) είναι τοποθετημένοι στην πλάκα, στις δοκούς θεμελίωσης και κατά μήκος των διαγωνίων των τοιχοπληρώσεων που υπόκεινται σε δυναμικές διεγέρσεις εντός επιπέδου. Η δυναμική διέγερση της σεισμικής τράπεζας θα βασίζεται στα δυναμικά χαρακτηριστικά και την σφοδρότητα του γνωστού καταστροφικού σεισμού της Θεσσαλονίκης (Βόλβης) του 1978. Με την κατασκευή από οπλισμένο σκυρόδεμα και τοιχοπληρώσεις, η GREENERGY στοχεύει να αποτιμήσει τη δυναμική δομική επιτελεστικότητα των παλαιού τύπου ανεπαρκών κατασκευών με το επόμενο παραδοτέο, D23. Η GREENERGY οραματίζεται την αστική δασοφύτευση υψηλής πυκνότητας, που υποστηρίζεται από καινοτόμες και ανθεκτικές ανακαινίσεις και παρακολούθηση της δομικής υγείας των κατασκευών.

Λέξεις κλειδιά: πείραμα, σεισμική τράπεζα, οπλισμένο σκυρόδεμα, τοιχοπληρώσεις, τούβλα, σεισμική διέγερση, Κάθετα Δάση, φυτό, ανθεκτικότητα, αναληπτικότητα, ανακαίνιση, δομικός, δομοστατικός, παρακολούθηση δομικής υγείας SHM, PZT

1 INTRODUCTION

GREENERGY conducts basic research at building level in order to review barriers in existing renovation approaches that lead to exclusion of forests from cities and detrimental incompatibility with built environment and revolutionize vertical forest (VF) concepts. It gathers and coordinates approaches and develops the fundamental structural and energy related drivers in order to allow for harmonic VF growth inside smart cities and interconnection of urban forests in a unified high-quality living environment for citizens. It defines critical parameters and suitable concepts in order to optimize resilient and safe ecosystem that combines existing concrete buildings/infrastructure and VF.

A physical model structure is going to be tested in lab to set proof of a)innovative concept as well as real time data collection to interact with digital twin (hybrid), b)suitable carbon neutral contributing structure renovation with green materials and c)suitable green corrosion-resistant building envelopes to act as a compatible structural interface with VF and allow its growth and advanced energy savings and high quality micro-climate.

Current renovation practices in the built environment fail to combine efficiently energy and structural retrofits in order to secure energy investments over time against potential hazards (earthquakes etc). The main reason is that most of basic research is fragmented to either energy or structural aspects and several crucial construction detailing are deficient. Further, they fail to incorporate green concepts and green, reusable, recyclable, natural strengthening materials in deficient buildings from a structural point of view as there is a lack in basic research that needs to prove the innovative techniques involved (such as structural ropes etc). Of the highest significance is the absence of a renovation vision that goes beyond the goal of temporary but relatively low economic savings and aims at the permanent high economic savings that are also nature-inclusive, real green, nature-powered, naturally controlled environment of sustainable building.

GREENERGY envisions forest diffusion to alleviate extreme weather conditions impacts in coastal seismic urban regions and to optimize inclusive people-centric social engagement towards habitant comfort and satisfaction, through high-density urban forestation starting from green- renovated buildings. Based on the poor state of the art in the field of renovation towards vertical forests and the great necessity for their urgent development, GREENERGY aims to really cope with detrimental climate change consequences and advance environmental resilience. In that aspect, the experimental quantification of the influence of critical parameters for green holistic renovation of common building to VF building with advanced structural, energy, forestry and habitant comfort performance is crucial. Therefore, GREENERGY addresses the following critical objective with D21 as follows:

-Design and construction of 3d as-built suitable reinforced concrete structure, of the test setup and instrumentation (cast with the specimen or external). Designs and photos of detailing and instrumentation of constructed as-built 3d structure.

2 STATE OF THE ART

Increasing urbanization, pollution of the environment require a more sustainable and friendly environment especially in cities. Suitable Vertical Forests may favor natural mechanisms for sustainable environment of high air quality, controlled humidity, satisfaction and comfort for habitants. The "vertical forests" are divided into several categories depending on the type and the way the plants are supported (Irga et al. 2023).

Since Ancient times Hellenic culture acknowledged “The Hanging Gardens of Babylon” as one of the Seven Wonders. Ancient descriptions refer to a man-made construction with ascending series of tiered gardens containing a remarkable variety of vines, shrubs, trees looking like a large green mountain. The Hanging Gardens' name is believed to refer to trees being planted on a raised structure such as a terrace.(Wikipedia 2022, Dalley 1993, Reade 2000, Foster 2004) It is worth mentioning that the first system of vertical greenery named "Vegetation Architectural Structure and System" was patented to Stanley Hart White in 1938 (Manouchehri et al. 2024).

Fig 2.1 The Hanging Gardens of Babylon painting. By Unknown author - http://www.plinia.net/wonders/gardens/hgpix1.html, Public Domain, https://commons.wikimedia.org/w/index.php?curid=65909

Despite the appreciation of ancient culture to “wonderful” urban gardens, most urban areas exclude forestry and someone may find only limited “ground garden oases” left unharmed and usually encircled by huge buildings, isolated by peri-urban forestry. Forests seem to be the most crucial “earth-lungs”. However, only limited research addresses the issue of high-density urban forestation (Marrug, 2018) even though the necessity and viability is demonstrated clearly in contemporary architecture since at least 2014 with Bosco Verticale in Milan [Wang and Gard). The idea of smart cities with high-density urban forestry through vertical forests (VF) to absorb in-situ high fossil fuel emissions, reduce pollution, energy consumption and urban heat island effect, increase biodiversity and habitant comfort has been proven at building level with Bosco Verticale and is believed a game changer in succeeding permanent Green Deal goals. Further, pioneering studies already conduct research on continuous monitoring of energy, air-quality, and comfort parameters on vertical green living walls (Helman et al., 2022).

VFs in newly constructed buildings, is easier to accommodate and realize. However, the real challenge in cities is to include the existing buildings stock. That is to utilize the already well-established economic investments for energy retrofit of buildings combined with structural retrofit (to protect the energy investment over time towards permanent economic and green savings, especially in seismic prone areas or coastal ones that mainly suffer from corrosion) and further integrated with game changer VF renovation. Following this combined approach the existing buildings deficiencies and vulnerabilities need to be addressed as well as to efficiently accommodate forestry.

The majority of civil engineering buildings are made of masonry or r.c. that are made of brittle materials (e.g. clay bricks, concrete). Regarding masonry, in the study by (Gioffre et al. 2022) the two basic techniques are presented, confined masonry and unreinforced masonry. After comparing the two techniques it appears that the confined masonry responds better to the earthquake. Weak R.C. frames with relatively strong brick wall infills may perform, in some cases, similar to confined masonry under dynamic loads. Joint materials used in reinforced concrete structural elements may be stiff. Then, the connections may sustain high load while their deformation capacity is relatively low. On the other hand, joint materials may be flexible sealants that can sustain high deformations while the bearing load in the joint is relatively low. Construction industry suffers a lack of suitable connectors in member joints that are both adequately flexible and may carry adequate load in several practical applications. Therefore, Polymer Flexible Joints (PFJ) that possess the hyperelastic characteristics of advanced polyurethanes may cover the technological gap (Rousakis et al., 2020). They may carry both adequately high loads and adequately high deformations. This results in remarkable reduction of detrimental stress concentrations due to high redistribution over a broader area of the bonding joint (Kwiecień et al., 2017, Kwiecień, 2014). Seismic resistant structures often suffer from unsuitable retrofits with stiff joint materials, resulting in undesirable micro-cracks initiation inside concrete or brick infill members (Kwiecień et al., 2017, Rousakis et al. 2020). Stiff, brittle mineral or epoxy grouts lead to stress concentrations and to marginal upgrade of structural response. Similarly, Composites externally bonded on brick masonry on concrete members using stiff adhesives limit the efficiency of retrofit due to the low substrate tensile-shear strength (Kwiecien et al. 2016, Tedeschi et al. 2014, Rousakis et al. 2020). The PFJ possess both higher tensile and shear capacity as well as higher deformability (higher damage energy), upgrade the performance of the jointed areas of brittle structural members, even beyond their elastic response and accumulation of damages (Kwiecien et al. 2016). Consequently, the structures reveal upgraded safety (Rousakis et al. 2020). PFJ can repair cracks by injection or filling structural gaps, to make flexible hinges (using polymers PM and PT) – polyurethane flexible joints (PUFJ), as well as bonding of composites using flexible adhesives (PS and PT) (Kwiecien et al. 2016) – fiber reinforced polyurethanes (FRPU). PFJs made of polyurethanes of various stiffness and deformability (e.g. polymers: PT – stiff, PS – middle stiff and PM – soft) can assure substrate compatibility for different loading and deformation requirements and for different joint substrates. All of them contribute in life protection and assure continuous safe structure occupancy. The application of this repair strategy in quick strengthening of infilled r.c. frames and its efficiency in improving the structural performance is not yet addressed. Yuksel et al. (2006) researched sprayable FRC ductile retrofit materials for application on deficient infill walls towards desirable inelastic response of RC frames, among several different intervention techniques addressed by other researchers (Rousakis et al. 2020). Fiber reinforced polymer sheet strengthening has been also investigated widely (Ozden et al. 2011). There were tested (Koutas et al. 2015) old-type deficient r.c. frames with infill walls strengthened with textile reinforced mortar. Under reversed, pseudo-seismic loading, the retrofitted infill walls showed rather fragile failure mechanism and behavior similar to the non-retrofitted ones. However, there was recorded relatively increased shear resistance and energy dissipation (Gams et al. 2017, Rousakis et al. 2020). There was severe accumulation of damage in the range of 0.5-1.5% lateral drift, limiting the potential of the retrofitted rc frames (Koutas et al. 2015). This aspect is crucial to the desirable ductile behavior of retrofitted infill walled frames to avoid uncertain effects of the infill walls that may lead to soft-storey mechanism (Fardis 2000, Rousakis and Tourtouras 2014) and potential whole-building collapses in cases of seismic induced overloads or out of plane collapse of infills. Externally bonded fiber reinforced polyurethanes (FRPU, see Rouka et al. 2017, Rousakis et al. 2020) applied on infills may contribute in broader engagement of the retrofitted brick infill walls in different bays and levels simultaneously, in terms of stiffness and shear force increase, of the deficient framed structures (see Rousakis and Tourtouras 2014, Rousakis 2016 for innovative rope retrofit of RC columns) at high inter-storey drifts.

On the other hand, Balsamo et al. (2005) provide a comprehensive experimental investigation of strengthening of a two-story construction with Carbon FRP (CFRP) laminates. The tests confirm that CFRP composite retrofitted structure may withstand a moderate earthquake. Garcia et al. (2017) present the effectiveness of using CFRP and Post – Tensioned Metal Straps (PTMS) in strengthening a full-scale building. The columns and joints of a two-story reinforced concrete building received innovative strengthening and it was subjected to seismic table excitations. Large scale dynamic testing is very important for the assessment of seismic resistant structures (Sharma et al. 2022). Recently concluded tests in seismic table by the PI together with a consortium of 8 universities and 3 private companies have demonstrated and validated the expected unique beneficial effects of the use of novel flexible polymers (INMASPOL SERA TA Horizon project) for retrofitting and repair of large scale structures (Hojdys et al., Rousakis et al. 2021) by using also NDT and DIC. Further, the PI has developed advanced analytical models of (digital twin) RC frames and structures with deficiencies, damages and innovative retrofits, within ESPA EDBM103 (MIS: 5050146) Horizon project (Rousakis et al. 2021a, Rousakis et al. 2021b) and INMASPOL (Hojdys et al. 2023).

The experimental study (Ali 2014) suggests that reinforcing concrete columns with coconut fiber ropes may be in some cases an effective and sustainable solution. Another type of ropes are the elastic polypropylene fiber rope (PPFR, products of Thrace Plastic Co. S.A, Greece). This type of rope shows extremely high deformability and can be effectively applied to reinforce columns without or with prestressing (Rousakis and Tourtouras 2014). Finally, FRP ropes (Golias et al. 2021, Karayannis et al. 2022, Karabini et al. 2023 & Karayannis et al. 2022) or Basalt fiber ropes (Rousakis and Macha 2023) or non polymer glued (Karantzikis et al. 2005, Triantafillou et al. 2006, Padanattil et al. 2017) or all-green reusable, recyclable, polymer-free and natural structural ropes used by the PI (Rousakis 2016, Rousakis et al. 2019) have been proven efficient enough in seismic resistant strengthening of rc joints, columns and beams. Joints have been one of the most critical members influencing the overall response of buildings during seismic events. Externally bonded FRPs have proven highly effective in enhancing the shear strength of joint panels, preventing shear failure, and thereby significantly reducing the overall risk to the building. Advanced alternatives offered with CFRP sheets, ropes and anchors (see Golias et al. 2021, Karayannis et al. 2022, & Karayannis et al. 2022, Del Vecchio et al. 2014. 2024a,, Karabini et al. 2023 among else) have been validated experimentally. Recently, the performance of critical anchor spikes in the overall behavior of the strengthening scheme was tested by Del Vecchio et al. 2024a, Del Vecchio et al. 2024b. Also, in terms of column reinforcement, it is worth mentioning the application of prestressed steel wire ropes embedded in polyurethane cement composite material (Guo et al. 2022). The analysis of this study shows that the seismic behavior of the columns improves after strengthening.

Maintenance and repairs costs of today's civil infrastructures systems, most of them constructed by reinforced concrete such as bridges, buildings of great importance, tunnels, tall buildings, is of major concern for the engineering community, as most of these are at or beyond their design life and the need to remain in service for an extended period is of profound importance. The use of a smart health monitoring system on new or old structures is even of greater importance, as the collection of reliable and consistent information will not only reduce the life-cycle cost but also provide information that will lead to an improved and safer design. Especially for reinforced concrete structures, developing innovative, low-cost, reliable techniques for real-time condition and damage assessment remains a challenge. The PZT transducers are compact, lightweight, small-sized and exhibit excellent SHM characteristics, such as a large range of linearity, self-sensing, fast response, low-cost, high conversion efficiency and long-term stability. In its recent research, members of the research team of this proposal successfully developed a PZT-based SHM system, WiAMS, for real-time condition and damage assessment in reinforced concrete structures. The focus of WiAMS Project is aimed at advancing autonomous structural health monitoring systems which could wirelessly transmit appropriate signals to ensure the state of structural condition of conventional and FRP strengthened concrete structures. In the frame of another research project, researchers study the consequences model and risk assessment on civil infrastructures, like bridges, buildings or infrastructures of great importance etc., using SHM technics. The operation and the feasibility of the wireless PZT-based SHM system in concrete members proposed by (Providakis et al. 2015, Providakis et al. 2016). It was experimentally validated in tested concrete members, reinforced concrete beams and frames by (Karayannis et al. 2015, Voutetaki et al. 2016, Voutetaki et al. 2022, Chalioris et al. 2020, 2021). Applications of the SHM system in RC beams have shown promising results concerning its effectiveness in detecting concrete cracking and steel reinforcing yielding in early damage levels (Karayannis et al. 2015, Voutetaki et al. 2016, Voutetaki et al. 2022, Chalioris et al. 2020). Relative research programs with the proposed research are the above projects:

2013 - 2015: «WiAMS Project: Development and Evaluation of a wireless real-time monitoring system for structural integrity assessment of concrete structures using a smart piezoelectric sensor network»

2020 - 2022: «Structural Health Monitoring of Fibre-Reinforced Concrete Elements using an Advanced System of Piezoelectric Transducers» European Union, European Social Fund Operational Programme: «Human Resources Development, Education and Lifelong Learning 2014- 2020».

2021 - 2023: «Risk and Resilience Assessment Center, Prefecture of East Macedonia and Thrace, Greece" which is implemented under the Action "Reinforcement of the Research and Innovation Infrastructure», funded by the Operational Programme "Competitiveness, Entrepre-neurship and Innovation" (NSRF 2014-2020) and co-financed by Greece and the European Union (European Regional Development Fund).

Several additional researches have been conducted on RC using the Electromechanical Impedance (EMI) method. Most of the work is focused on SHM and damage detection in RC members subjected to monotonic loads (Ai et al. 2018, 2019) and in RC members subjected to corrosion (Talakokula et al. 2014, Talakokula and Bhalla 2015). Concerning the seismic risk, only a few published works deal with the monitoring of shear and seismic compressive stress in concrete, shaking table test of a one-bay-two-storey RC frame (Hou 2017). Taking into account the lack of research or demonstration projects on renovation of existing buildings to VF ones, GRENERGY will address the gaps in fundamental research concerning: i) the region- and building dependent forestry, ii) the suitable structural joints and anchors or additional constructions and suitable interfaces to accommodate and grow over time forestry on the existing building, iii) the efficient seismic retrofit of the common deficiencies of existing buildings with the forestry additional mass and detailing included, iv) the continuous smart PZT monitoring of the system with digital twin model that allows the investigation of key parameters and examination of different scenarios. The consortium as a whole has the required expertise in different aspects of forestry, experimental investigation of novel seismic retrofits, numerical modelling and monitoring of structures, thus enabling an effective integration of the potential research challenges associated with the targeted breakthrough. Also, connection to previous and ongoing European research projects (e.g. INMASPOL project, WiAMS project, RiskAC NSRF project) may constitute as a reference, while the project aims at developing a more advanced approach in order to address a ground breaking concept in green renovation of existing buildings taking into account the combined effects of forestry and structural retrofits in seismic prone areas.

If we consider that: i) by 2030, 60% of the global population is projected to live in urban areas, ii) cities consume 75% of the world's natural resources and account for more than 70% of global CO_2 emissions, iii) cumulative emissions of CO_2, together with methane and other greenhouse gases, largely determine global mean surface warming of the planet, causing ice melting, biodiversity loss and rising sea levels (urban forestry manifesto, https://www.stefanoboeriarchitetti.net/en/urban-forestry/) and on the other hand that: i) forests and trees – which are at risk of continuous erosion all over the world – absorb nearly 40% of fossil fuel emissions largely produced by our cities every year, ii) leaves and roots of a mature tree absorb CO_2 through photosynthesis and help reduce the pollutants (responsible for a high percentage of respiratory diseases and premature deaths) present in the air then if a single tree can bring great benefits to the city and its inhabitants, an urban forest can be an extraordinary help to improve the quality of health and life in a city (https://www.worldforumonurbanforests.org/). We believe the impact of the forestry-inclusive renovation alone will be huge. Furthermore, the proposed structural retrofit innovations will enable for the rapid urban forestry development, lifting most crucial contemporary barriers. The structural retrofit innovation proposed herein responds to the lack of suitable structural solutions in civil engineering, related to creation of structural connectors based on bonding, having ability to transfer loads and high deformation simultaneously. Moreover, the peaks of stress concentration in brittle materials are responsible for their weakening, especially, when a stiff joint between two brittle structural elements is working. This is the case when stiff and brittle mineral or epoxy grouts are used as repair injecting or as adhesive (matrix) in composite strengthening. In seismic areas, high amount of ductility and deformation capacity of structures are required. Damaged (cracked) structures manifest low resistance to acting loads, thus protection, repair and strengthening methods should not only recover prior resistance but also introduce advanced, safer structural behavior. It is required from constructions that they will be able to deform safely and largely under extreme loads. Advantageous reduction of stress concentrations and required deformability is assured only by highly flexible systems made of special polyurethanes (PUFJ and FRPU). This new kind of flexible joint introduces greater tensile and shear resistance, deformability and ductility (greater bearing capacity) into the bonded brittle structural elements, also in the post failure deformation zone - making the structure safer. Broader structural and energy impact: Concrete frame buildings with masonry infill are not only numerous in residential dwellings but are often the preferred typology of strategic buildings such a hospitals, schools, police and fire stations, rescue teams headquarters.

These buildings often have to be rapidly shored and partially retrofitted reliably – no matter the cost - (especially if they have light to heavy damages in nonferrous elements such as infills) as their role in community resilience as a whole is huge and an 'out of order period' may lead to total failure of the state services to respond according to emergency plans and save human lives. Therefore, consequences of damage to these buildings are very significant, with manifold aspects impacting on private lives as well as working lives and other activities (Fig. 2.2, 2.3).

By reducing the damage to dwellings, and with effective green retrofit of deficient RC members and forestry inclusion, the GREENERGY project aims at limiting this additional huge burden. Simultaneously, both the energy and forestry retrofits are protected and sustainable full functionality is secured over the whole life-cycle through smart monitoring. The physical-digital twin structure will serve as demonstration to stakeholders and students after completion of GREENERGY and will allow for the investigation of future critical scenarios. Similarly, the developed structural health monitoring system may be used also in buildings of great importance, highway structures, bridges and parts of reinforced structures which are not accessible.

Figure 2.2. Typical damage observed on in-plane infill masonry walls: (a) detachment of the surrounding RC frame in the L'Aquila (Italy) 2008 earthquake; (b) diagonal cracking in Lorca 2011 (Spain) and (c) in the Nepal 2015 earthquake and (d)–(e) Kefalonia 2014 (Bournas 2018) .

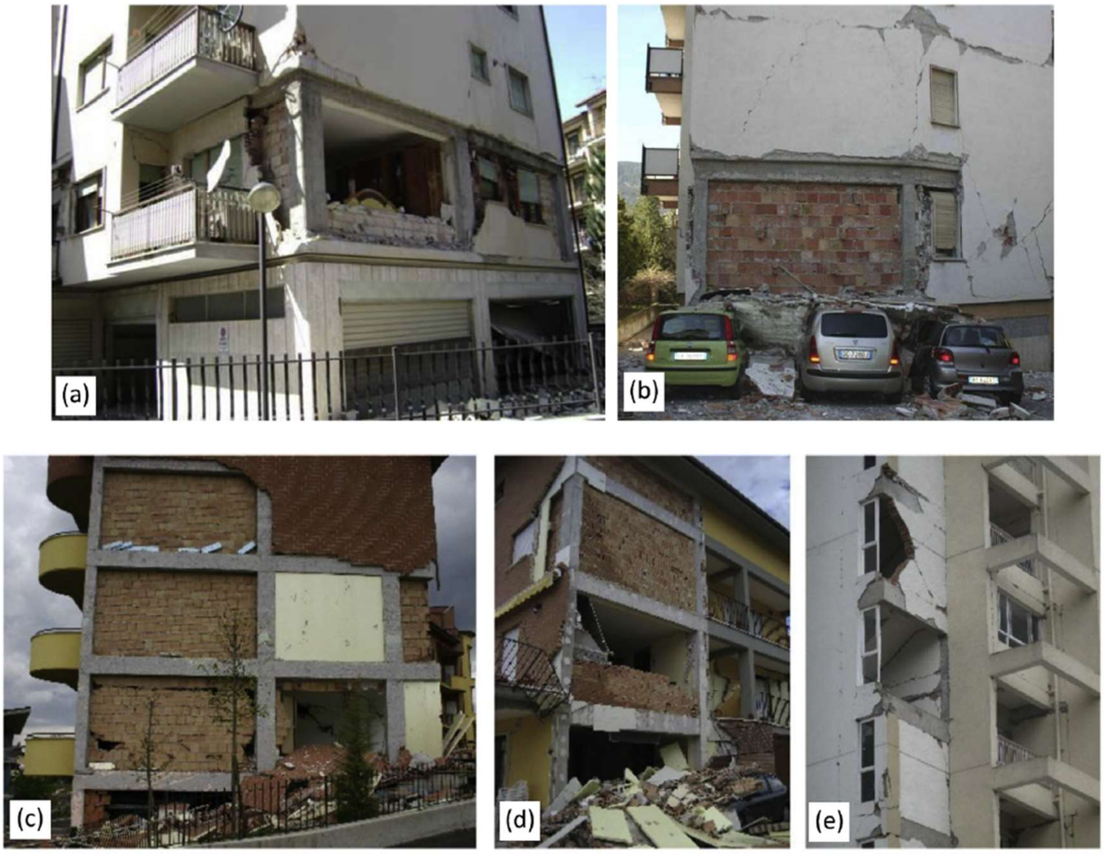

Figure 2.3. Example of out-of-plane collapse of masonry infills in RC multi-story buildings: (a)–(d): L'Aquila 2008, Ms 6.3 and (e) in the Nepal Earthquake in 2015 (Bournas 2018).

2.1 METHODOLOGY

The maximum utilization of natural mechanisms through VFs for sustainable environment of high air quality, controlled humidity, satisfaction and comfort for habitants is the main global objective.

The experiments cover design, construction, instrumentation, testing and assessment of performance of 3d VF structure towards holistic renovation.

The overall objective is to quantify experimentally the influence of green holistic renovation of common building to VF building with advanced structural, energy, forestry and habitant comfort performance.

To meet the objective of D21 and to reach the main target of the development of the VFs in efficiently renovated buildings combining structural, energy and forestry retrofits, various procedures and methodologies are utilized associated with the following component:

construction of physical model as-built structure to test under dynamic loading in lab. It includes design, construction, as well as innovative PZT instrumentation. The whole construction itself will be an innovative hub for continuous monitoring and crucial results acquisition over the implementation of the following D22-D26 deliverables, as well as beyond the termination of GREENERGY project and will serve as demonstration basic research project in DUTh lab.

The structure: One fully symmetrical 3D frame of one storey with 4 RC columns, 4 beams, a slab and 4 infill masonry walls is constructed, all designed according to old generation guidelines. The building generally follows the morphology of INMASPOL real scale building https://serata.eucentre.it/index.php/sera-ta-project-37/ in which the PI was leader of the team conducting the experiments (see i.e. Rousakis et al. 2020) and it is scaled down to the capacity of DUTh lab seismic table capacity (see section 3.1.1.2).

Structural health monitoring for real-time condition and damage assessment in the constructed concrete structure is performed with PZTs. Prompt damage diagnosis of seismically deficient VF buildings requires, in addition to the other common testing measurements, the monitoring and evaluation in a real-time system based on piezoelectric sensors or piezoelectric transducers (PZTs). This innovative Structural Health Monitoring (SHM) system uses sensors as an embedded-in smart aggregate featuring smart properties or implementing a network of piezoelectric patches monitoring the condition of the reinforced concrete structure. The SHM system is based on the Electro-Mechanical Impedance (EMI) sensing method utilizing the voltage signal measurements of a series PZT transducers mounted to the structure. EMI-based SHM method utilizes piezoelectric patches, which are mounted adequately to the structure by a robust bonding interface. Piezoelectric patches can operate as (a) actuators to vibrate the inspection area of the structure in terms of mechanical wave with high frequency excitations (converse piezoelectric effect), and simultaneously as (b) sensors to monitor the changes in their electrical impedance due to the impedance of the structure (direct piezoelectric effect).

This report focuses on the advanced design of the suitable as-built, scaled-down reinforced concrete structure, of the test setup and of the instrumentation (cast with the specimen or external). It includes detailed presentation of the construction of the structure, of the test setup and of the instrumentation.

3 AS-BUILT 3D STRUCTURE

3.1 SEISMIC TABLE CHARACTERISTICS

A shake table simulates the ground motions that take place during an earthquake. They're used to test structural models, scaled slopes, or building components, typically to the point of failure. In the seismic table, the behavior of simple indicative types of buildings is approximated. The user can vary the intensity of the two horizontal and also the vertical component of the earthquake and detect the qualitative difference of the results. Also, the variable vulnerability of the models to seismic excitation is noticed. Buildings with many openings, with extreme height and with irregularities (plan, section or infill presence etc) prove to be relatively vulnerable than more symmetrical ones.

In this section, a brief reference will be made to major seismic tables that contribute to the experimental breakthroughs around the world. Their basic characteristics such as: table size, maximum load, maximum displacement, etc are discussed.

3.1.1 Characteristics of existing seismic tables around the world

Shake table E – defence) (Miki, Japan, Asia)

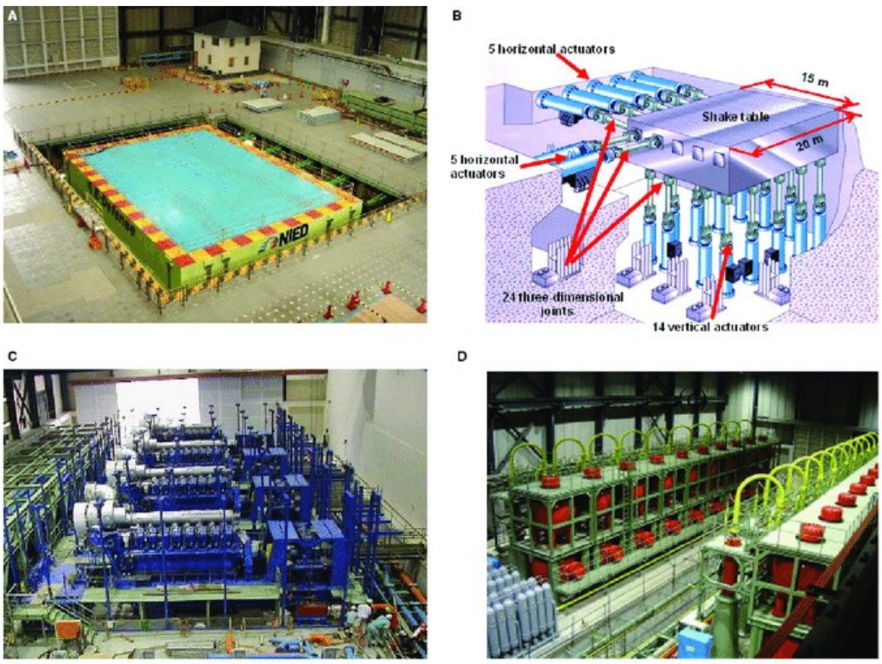

Figure 3.1 Shake table of Japan (Nakashima et al. 2018)

The world's largest 3D full-scale earthquake experimental simulation, named E-Defense, was built by the Japanese government's Science and Technology Agency and operated by Japan's National Research Institute for Earth Science and Disaster Resilience (NIED). This shake table has a table size of 20 x 15 m and can carry a load of 12MN. Also the maximum displacement is ±1 m along the x and y directions, while it is ±0.5m for the z direction. It is important to mention that the maximum acceleration under the maximum loading is $9m/s^2$ and $15m/s^2$ for x,y direction and z direction respectively.

The seismic simulator is driven by 5 horizontal actuators installed in each direction and by 14 vertical actuators. Large joints are installed at the connections between the table and the actuators, allowing three-dimensional movement with minimal friction. Actuators can produce a frequency of 15 to 30 Hz (Nakashima et al. 2018).

Shake table at the university of California (Berkeley, California, USA)

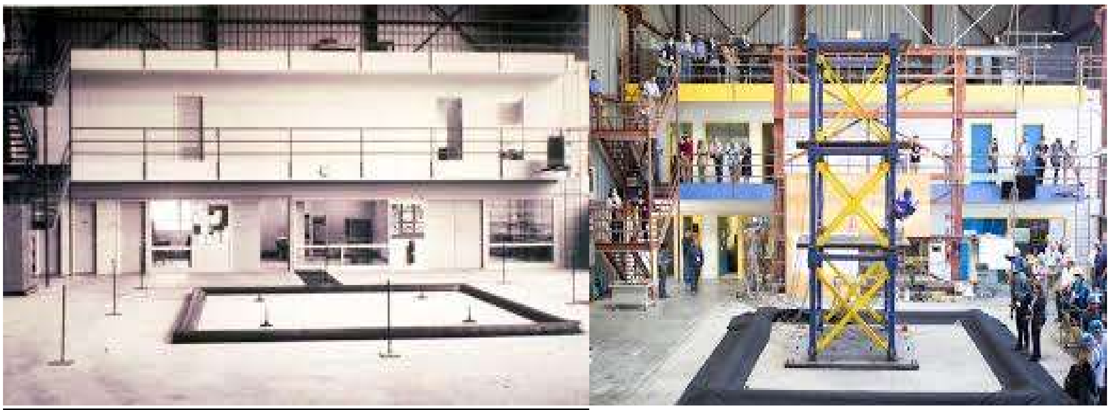

Figure 3.2 Shake table of Berkeley (https://peer.berkeley.edu)

The seismic simulator at the University of California, Berkeley, is one of the largest in the United States. The dimensions of the steel table are 6.1 x 6.1 m. It has a total of six degrees of freedom with movements around the three axes X, Y, Z. It is important to mention that the 45-ton steel table can develop a maximum acceleration of 1.5g with a maximum payload of 45 tons. The velocity it can develop is maximum 0,76 m/s. Also, the maximum peak displacement is ±0,125m. The frequency ranges between 0 and 15 Hz. The seismic table is moved by eight hydraulic actuators in the X and Y directions, while in the vertical direction by four hydraulic actuators

The University of Berkeley, in addition to the triaxial seismic table, also has a 2.1 x 5.8 meters single degree of freedom simulator. This system has the ability to support projects that require a large displacement, as the maximum displacement that can be reached is 0.5 m (https://peer.berkeley.edu/uc-berkeley-shaking-table-history)

.

Shake table Azalee (CEA Saclay, France, Europe)

Figure 3.3 Shake table of CEA Saclay

France's seismic table AZALEE, which is part of the TAMARIS facilities, belongs to the CEA Seismic Laboratory. ((EMSI)) It is a seismic simulator with an area of 6.0 x 6.0 square meters and a mass of 25 tons. The excitation axis of the simulator is triaxial (XYZ) and for this reason it can develop 6 degrees of freedom. The AZALEE seismic table is used for testing samples up to 100 tons. Thus, depending on the mass of the sample, the corresponding accelerations are applied to each axis, with maximums of 1g and 2g in the horizontal and vertical directions respectively. The velocity it can develop is maximum 1m/s. Also, the maximum peak displacement is ±0,125m. The frequency ranges between 0 and 100 Hz. The maximum building height it can receive is 12 m.

Tests are carried out with the help of eight hydraulic actuators, 2 in the X and Y axes and 4 in the Z axis. Each of these actuators can develop a maximum force of 1000 kN on the excitation table.

Shake table at the University of Buffalo) (Buffalo, New York, USA)

The Laboratory of Structural Engineering and Earthquake Simulation of the University of Buffalo, USA, has two square earthquake simulators with a surface area of 13 square meters. Two high-performance, relocatable, six-degrees of freedom shake tables are located in a trench along the north wall of the main laboratory. The tables can be controlled either independently or as a single, synchronized table. Synchronized table motions can be fully in-phase or uncorrelated. Together, the tables can support specimens weighing up to 100 metric tons with a length up to 120 feet. The equipment to operate these shake tables include a high-capacity, high-performance hydraulic supply and controller along with numerous digital control systems.

Figure 3.4 Shake table of Buffalo (https://www.buffalo.edu)

The tables are designed with the following theoretical performance:

A 3.6 x 3.6 meters table platform of welded steel construction with a weight of approximately 12 tons. The table has a painted top surface. A 7 x 7 meters shake table extension platform of welded steel construction with a weight of approximately 9.8 tons. The extension has painted top surface. The maximum load it can carry is mass specimen 50 tons maximum and 20 tons nominal. If we use the table extension platform in place, the maximum overturning moment is 46 tons meter. Maximum off center loading moment is 15 tons meter. The shake table operates on frequencies between 1-50 hertz nominal to 100 hertz maximum. The velocity is between 500 mm/s to 1250mm/sec. (https://www.buffalo.edu/seesl/services/shake_tables.html).

Shake table at the institute of IZIIS (Skopje, North Macedonia, Europe))

The seismic table is located at the Institute of Earthquake Engineering and Engineering Seismology (IZIIS, Skopje). (Skopje, 1965) The dimensions and weight of the pre-stressed reinforced concrete slab on which the specimen is placed are 5.0 x 5.0 meters and 30 tons respectively. The maximum payload that can be tested in this particular seismic simulator reaches 40 tons. It has five degrees of freedom with movement in the horizontal and vertical direction. The maximum displacement and acceleration in the horizontal direction are ±125mm and 3g respectively, while in the vertical direction they are ±60mm and 1.5g respectively. The speed it can develop in both directions can reach 1m/s in the horizontal direction and 0.5m/s in the vertical direction. The frequency range of the system is 0-80 Hz.

Figure 3.5 INMASPOL structure on the shake table of Skopje (https://www.iziis.ukim.edu)

Shake table at the National Technical University (Athens, Greece, Europe)

The seismic simulator of the Anti-Seismic Technology Laboratory of the NTUA consists of a rigid platform with an area of 4.0 x 4.0 m and a payload of about 10 tons. Shake table has six degrees of freedom. Consists of 8 hydraulic pistons, two horizontal in the X direction, two horizontal in the Y direction and four hydraulic pistons in the vertical Z direction. In the vertical Z direction, in addition to the four hydraulic pistons, it also has a pneumatic piston. The maximum transport acceleration that the simulator can develop in the two horizontal directions is 2g, while at the same time in the Z direction it is 4g. The movement during the operation of the seismic table reaches ±10 cm, as well as the velocity of 1 m/s.

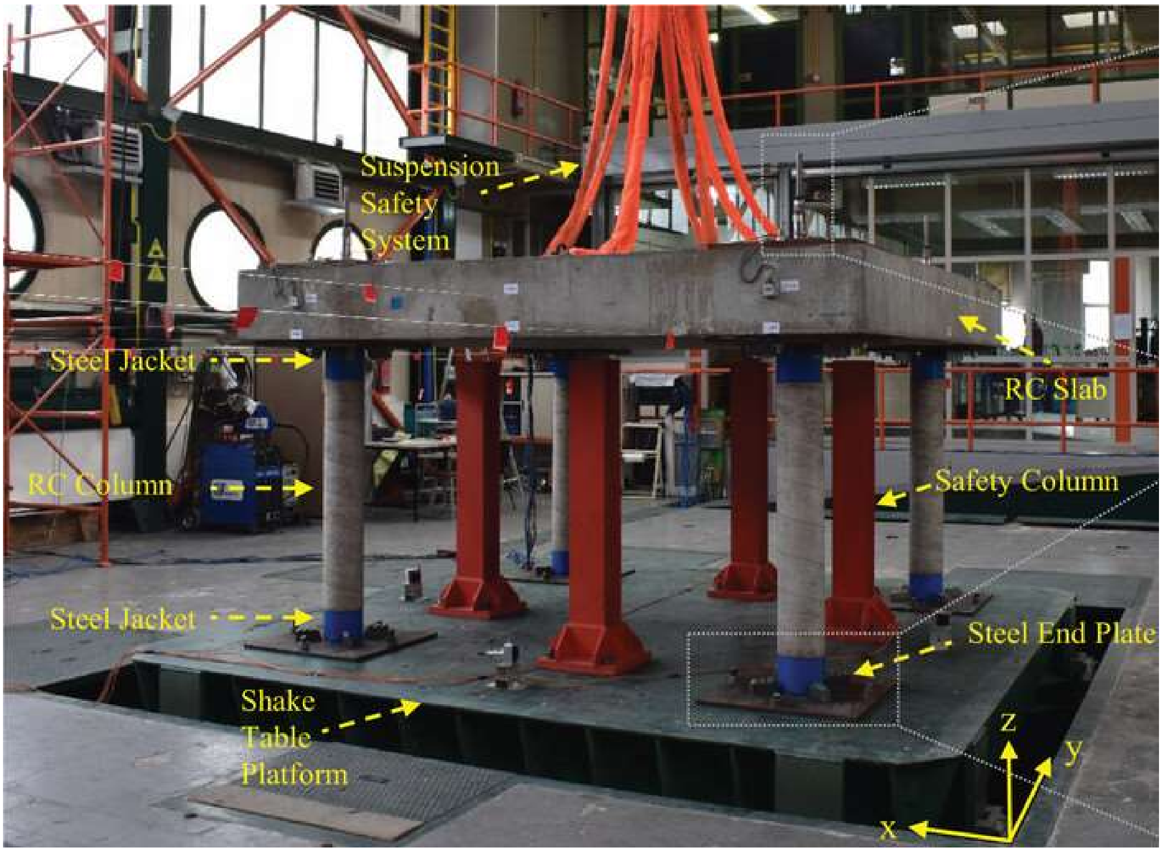

Figure 3.6 Shake table of NTUA, Athens (Katsamakas et al. 2024).

The seismic simulator is controlled by an analog system, which in turn is controlled by a digital system using a computer. The surface motion of the seismic simulator can be a sinusoidal excitation, a random motion, or even a real or even artificial earthquake.

Shake table at the Tongji University (Shanghai, China, Asia)

Single Shake Table

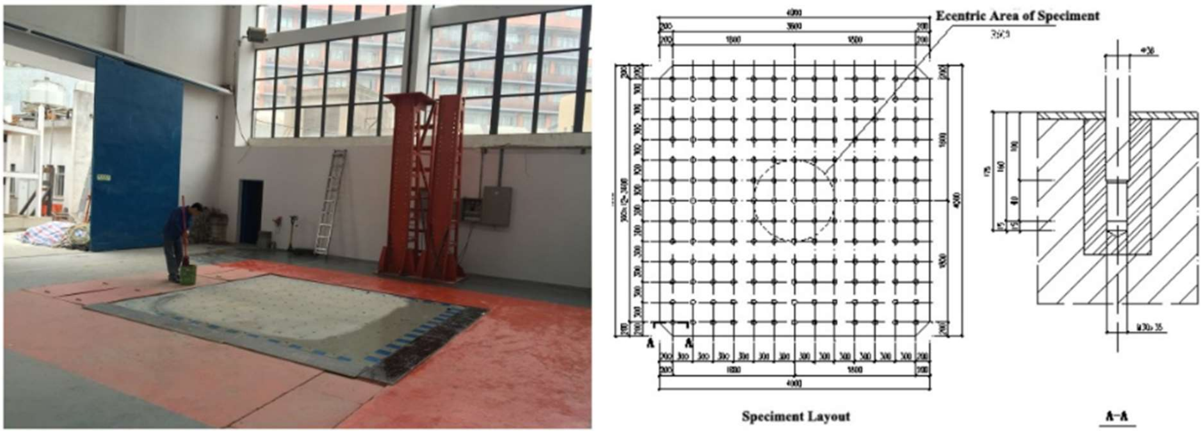

Figure 3.7 Shake table of Shanghai

The seismic table available at the University of Tongji is MTS shaking table. The shake table has 6 degrees of freedom. The dimensions of steel plate are 4m x 4m. It has six degrees of freedom and it works at 0,1 – 50 Hz of frequency. It can take 25 tons maximum payload. At the direction x the max acceleration is 1,2g, max velocity 1000m/s and max displacement 100 mm. Respectively at the direction y max acceleration is 0,8g, max velocity 600m/s and max displacement 50 mm. Finally at the direction z max acceleration is 0,7g, max velocity 600m/s and max displacement 50 mm.

Multi-Function Shake Table

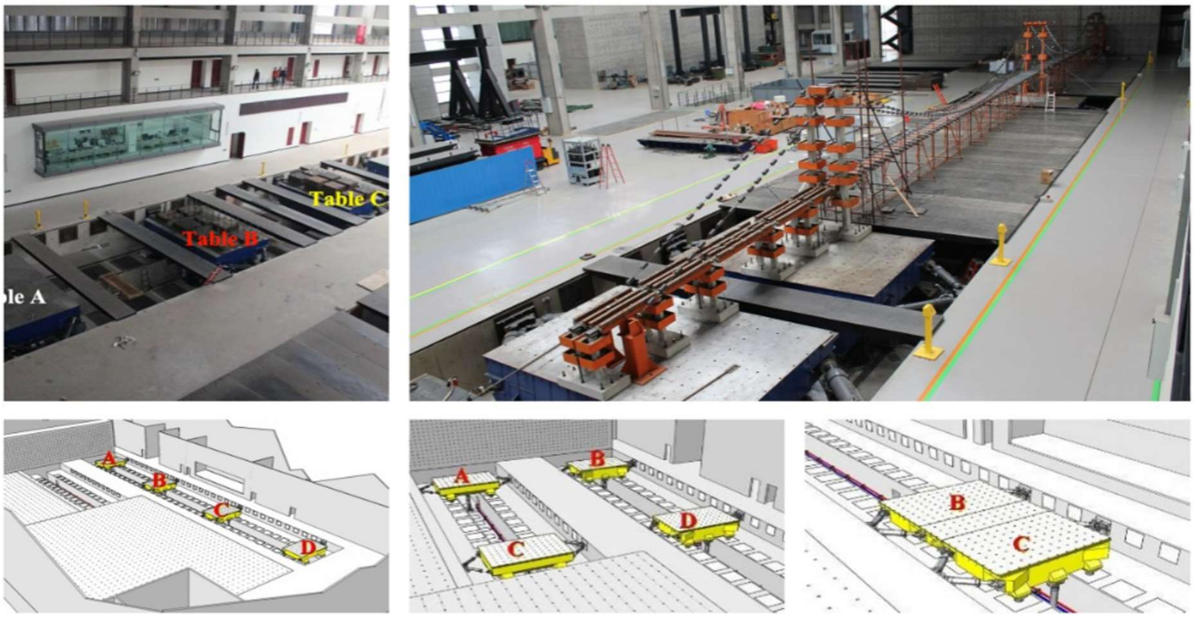

Figure 3.8 Shake table of Shanghai

At the University of Tongji there is a Multi-Function Shake Table Array. The multi – functional shake table consists of four 6mx4m shaking tables and one reaction wall. Each of the table has two horizontal translation degrees of freedom. The tables are situated in two trenches. Shake tables operate by groups: A with D and B with C. The displacement that shake tables can take is 500mm both horizontal directions. Some other characteristics for multi-function shake table are the velocity (1000mm/s both horizontal directions), acceleration (1,5g both directions) and frequency (0,1 – 50 Hz).

Shake table at the University of Bristol (Bristol, England, Europe)

Figure 3.9 Shake table of Bristol (Di Michele et al. 2023).

The shaking table has dimension of 3m by 3m, powered 8 hydraulic pistons. The payload is 15 tons and the maximum acceleration 1.5g (for lower payload). Maximum displacements reach ±150mm. The seismic table is supported inside a strong reinforced concrete well with 300 tons mass. The pit area is isolated from the rest of the laboratory by a 20mm gap that is filled with cork.

The hydraulic power is supplied by a group of 6 hydraulic pumps with total combined capacity of 900 litres/min at a working pressure of 205 bar. The maximum flow capacity can reach 1200 litres/min for up to 16 seconds during high demands through extra hydraulic accumulators. The vertical pistons are connected directly to the reinforced concrete block well and to the seismic table. They have a special static section to carry the total load of the table and of the specimen. Each vertical or horizontal dynamic piston may reach 70 kN capacity and a stroke of 300 mm.

3.1.1.1 Special characteristics of DUTh Seismic Table

Shake table at the University of Democritus (Xanthi, Greece, Europe))

The seismic table available at the Laboratory of Reinforced Concrete and Seismic Design of Structures of D.U.Th. is of ANCO R-643A type. The dimensions of the steel table are 3.4 x 3.4 m, while its total payload is 8 tons and 8 tons meters. It has two horizontal pistons with a capacity of 10 tons each. The maximum displacement of the seismic table reaches ±13 cm and ±15 cm for dynamic and static loading respectively. Depending on the mass under excitation, the acceleration of the seismic table reaches 1.6g for 8 tons or 2.9g for 4 tons. The maximum velocity that can be developed, as well as the frequency range are 1.2 m/s and 0-50 Hz respectively.

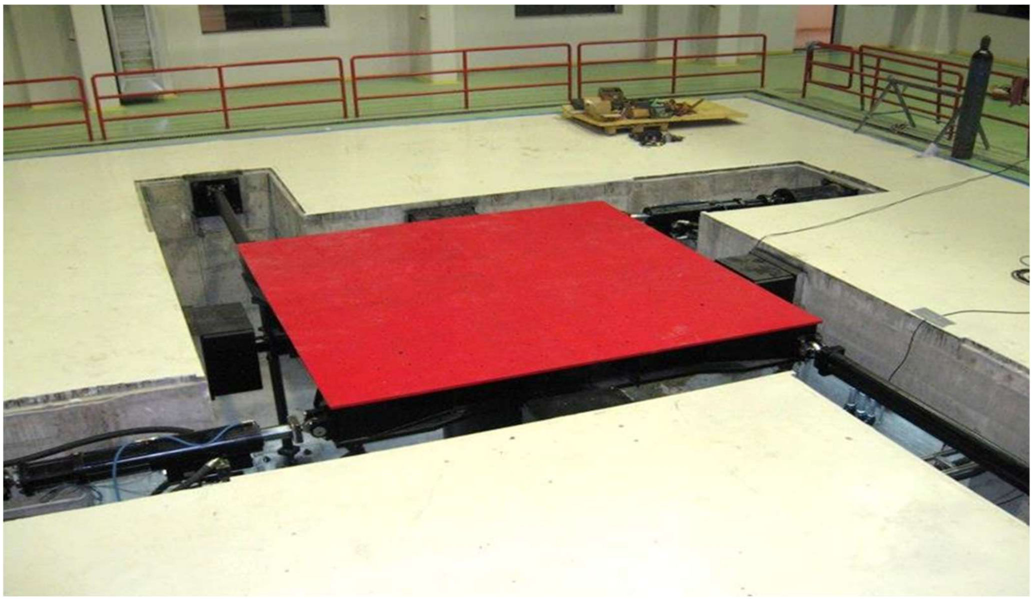

Figure 3.10 Shake table of DUTh, Xanthi.

The servo controller features an internal analog displacement loop controller with PID control and a computer based single axis external loop controller with filter data acquisition system. The seismic table has two Dytran piezoelectric accelerometers, with cable and preamplifier, one for controlling the movement of the table and one for specimens located on it. The tests use a dynamic construction monitoring system consisting of 16 uniaxial accelerometers of high resolution and sensitivity. Finally, the operation and control of the seismic table systems is carried out by the special control room. (Karabinis et al., 2008)

3.2 DESIGNS AND PHOTOS OF DETAILING AND INSTRUMENTATION OF CONSTRUCTED AS-BUILT 3D STRUCTURE

3.2.1 Test specimen

One fully symmetrical three dimensions (3D) structure of one storey with four (4) columns, 4 beams, a slab and 4 infill masonry walls is constructed, all designed according to old generation guidelines, before the introduction of Eurocodes or new Greek seismic code. That is, the structure includes RC columns with sparse steel stirrups and absence of capacity - based design that results in column-relevant detrimental damages. The brick wall infills include old – type clay bricks with horizontal holes and relatively low strength bonding mortar. The top layer of bricks is built inclined to increase the bonding to the top slab, according to old traditional practice. The building is scaled down to the capacity of the DUTh seismic table that can perform with a maximum mass of tested structure of 8 tons and 8tn*m maximum overturning moment (see 3.1.1.2). The scaled structure has plane dimensions of 2.70 × 2.70 m and total height of 1.95 m based on the detailing of the anchoring system of the seismic table of Democritus University of Thrace (DUTH) (Fig. 3.11, 3.12, 3.13). Two holes of the same diameter are made at each end of the foundation beam. The height to the level of the diaphragm is 1,57 m (Fig. 3.17).

Initially the foundation consists of four foundation beams. The cross-section of the foundation beams has dimensions of 0.25*0.2 m (height, width, Fig. 3.13, 3.17). The foundation is reinforced with 8Φ14 mm longitudinal bars (3 bottom, 3 top and 2 middle bars) and transverse reinforcement Φ10/100 mm stirrups (Fig. 3.25). The four columns (Fig. 3.14) and the infill rest on the foundation. The clear height of the columns below the slab is 1m. The height of infills is similarly 1m (Fig. 3.17). The length of the infills along the direction of the excitation (in plane loading) is 0.3 m, while the length of infills along perpendicular direction is 1.24 m. The masonry is made of clay bricks with dimensions 60/90/190 mm (width, heigh, length) (Fig. 3.15, 3.17, 3.18). The columns are reinforced with 4Φ8 longitudinal corner rebars and Φ5,5/60 mm stirrups (Fig. 3.25, 3.26). On top of the columns a RC slab with thickness of 20 cm is constructed, at 1m height from the foundation. The slab is extended beyond the frame beams (hidden inside the slab thickness) to provide sufficient top and bottom surfaces for the future attachment (anchoring) of vertical forest constructions (on internal and cantilever slab regions, see Fig. 3.16). Further, the solid slab-diaphragm provides most of the top mass of the structure that is necessary to lead to the damage of the as-built structure, mainly the columns and the brick wall infills. Of course, additional steel mass rods may be attached on the top of the slab to increase the top mass if required. The slab is reinforced with Ø8/100 mm at the top and at the bottom (Fig. 3.24). There is additional end-anchorage reinforcement at the perimeter edges of the slab. The slabs are supported by the four top hidden beams. More specifically, the hidden beams are reinforced with 8Φ10 longitudinal reinforcements (3 bottom, 2 middle and 3 top bars) and Φ10/100 mm transverse reinforcement, i.e. stirrups. The columns above the slab are 0.5m high, with identical longitudinal reinforcement 4Φ8 and transverse Φ5.5/60 mm. Finally, it is important to mention that the scaled model structure is constructed on a special beam foundation, with provided holes for attaching the whole structure to the shake table (Fig 3.12, 3.13) as well as steel hooks on the slab for lifting and manipulating the structure.

Figures 3.13-3.26 show in detail the design and construction of the reinforced concrete structure.

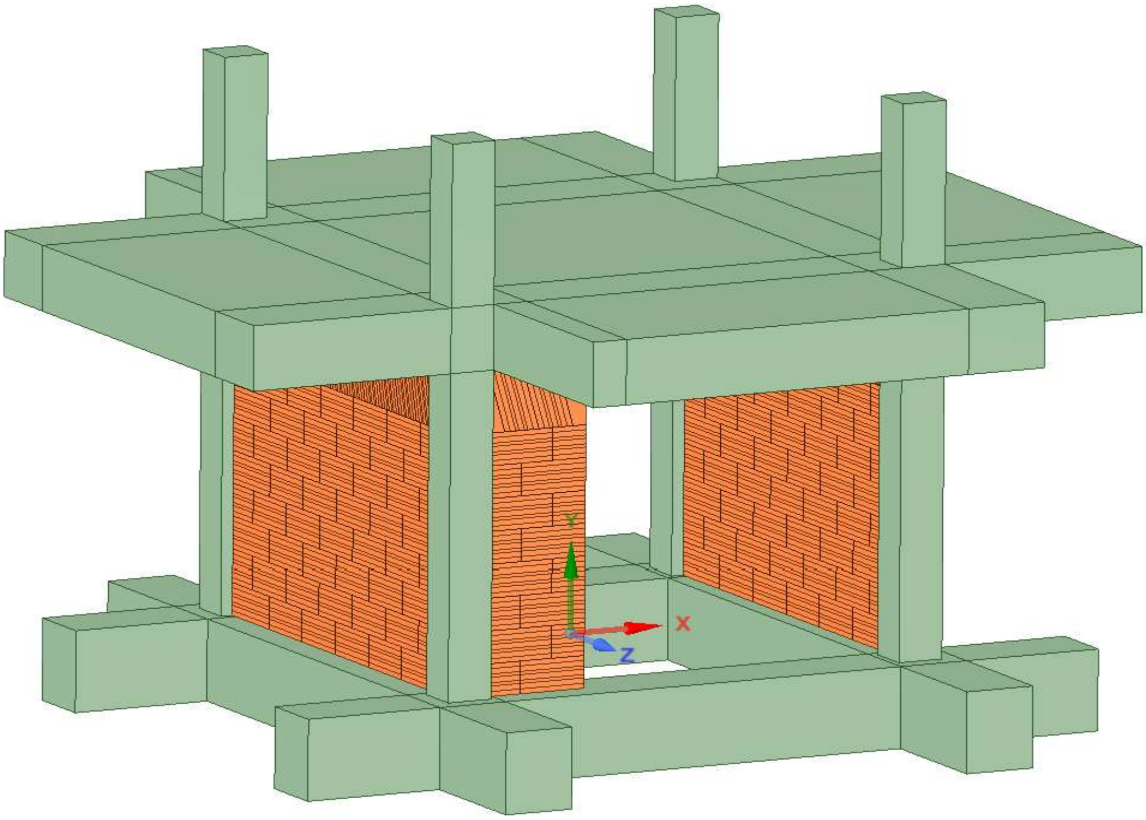

Fig. 3.11 3D View of construction

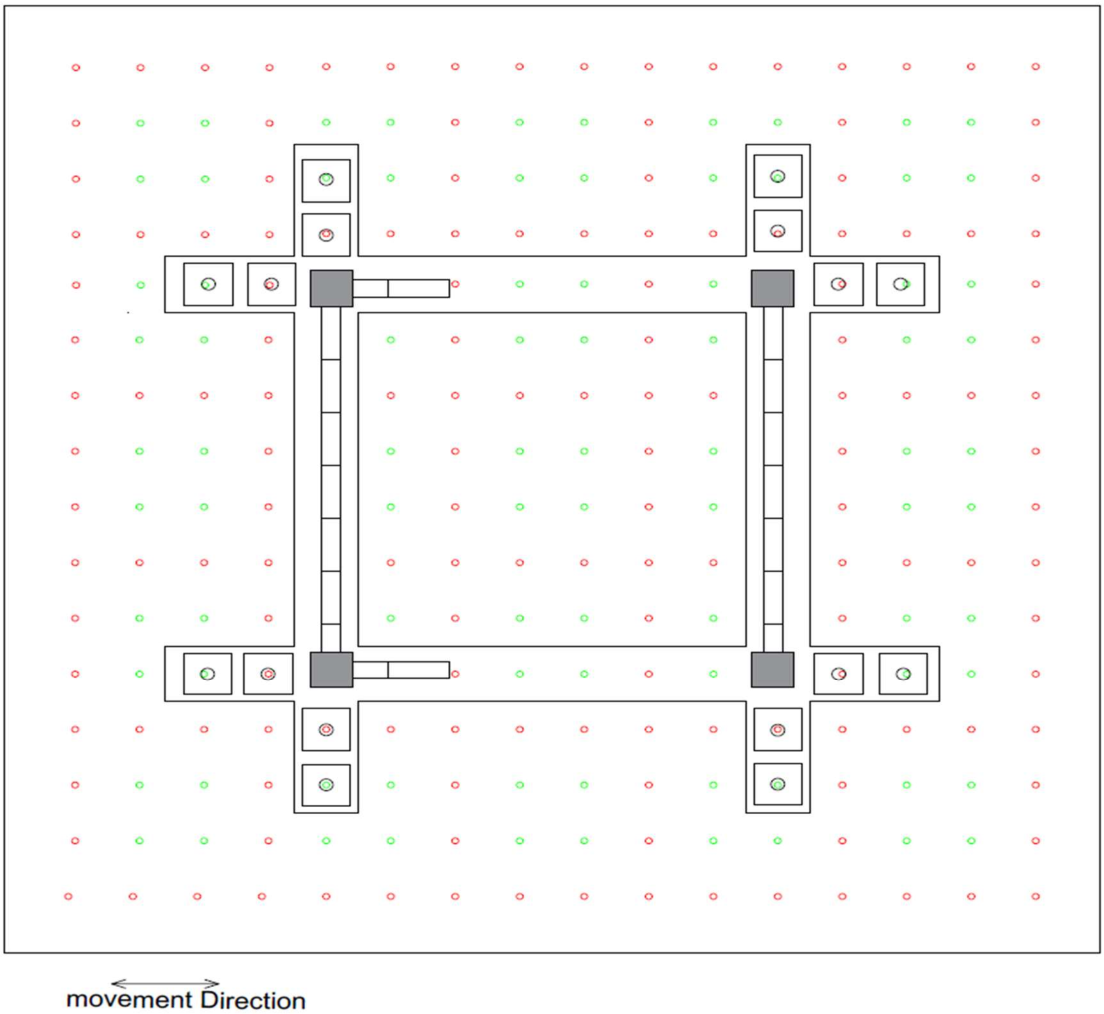

Fig. 3.12 Construction on the Shake table

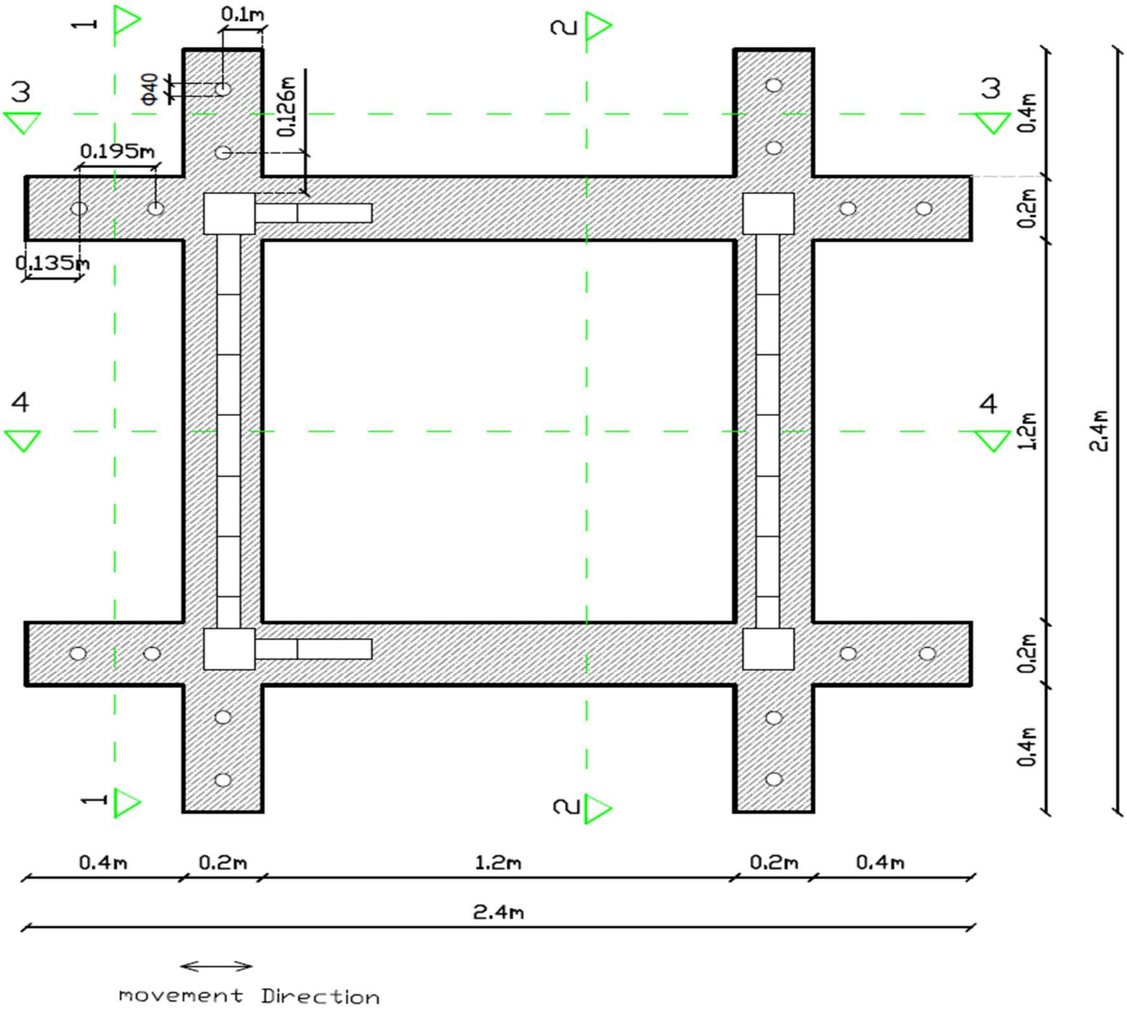

Figure 3.13 Floor plan of foundation

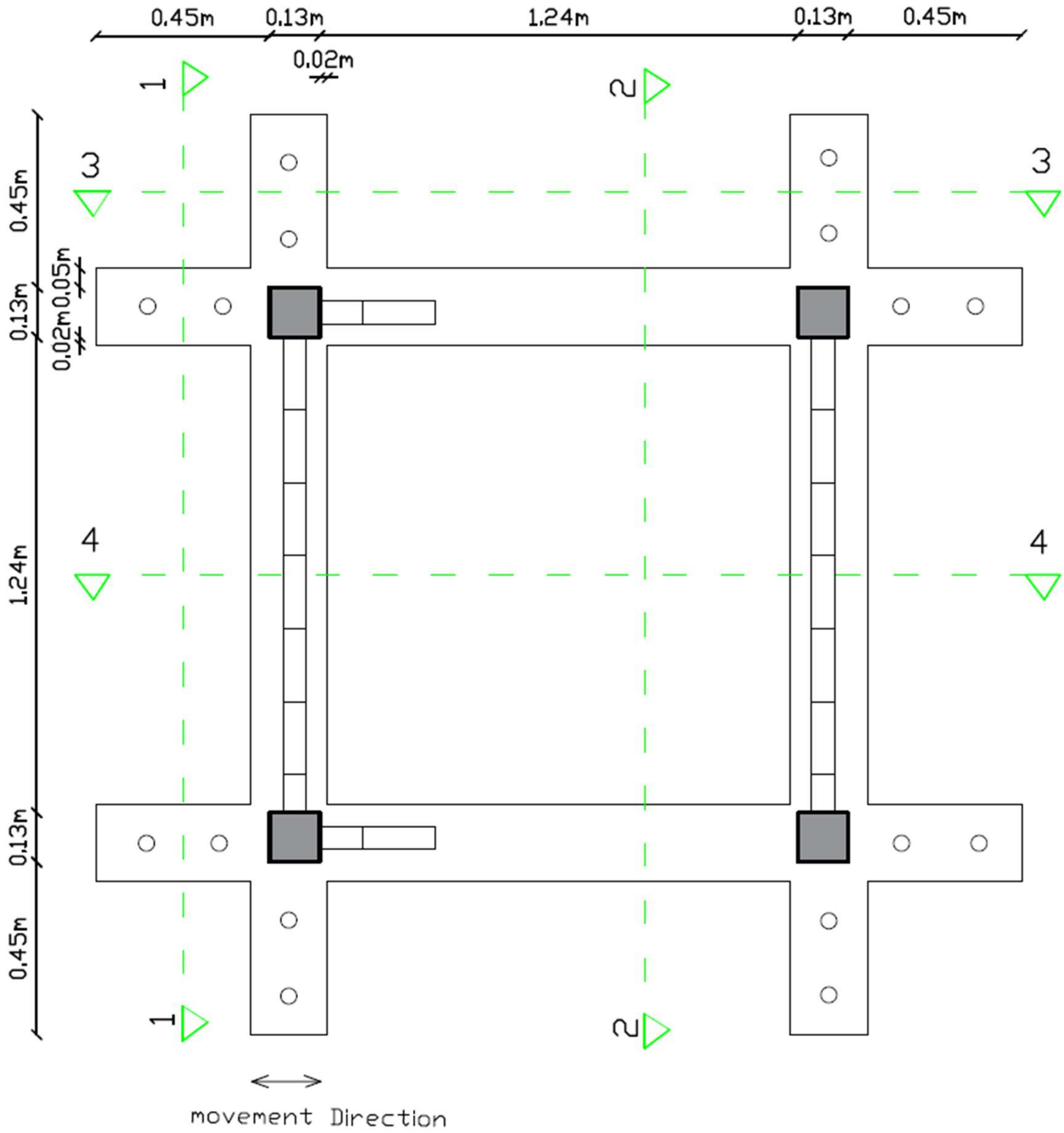

Figure 3.14 Floor plan of columns

H.F.R.I. Hellenic Foundation for Research & Innovation
Greece 2.0 NATIONAL RECOVERY AND RESILIENCE PLAN
Funded by the European Union NextGenerationEU
GREENERGY

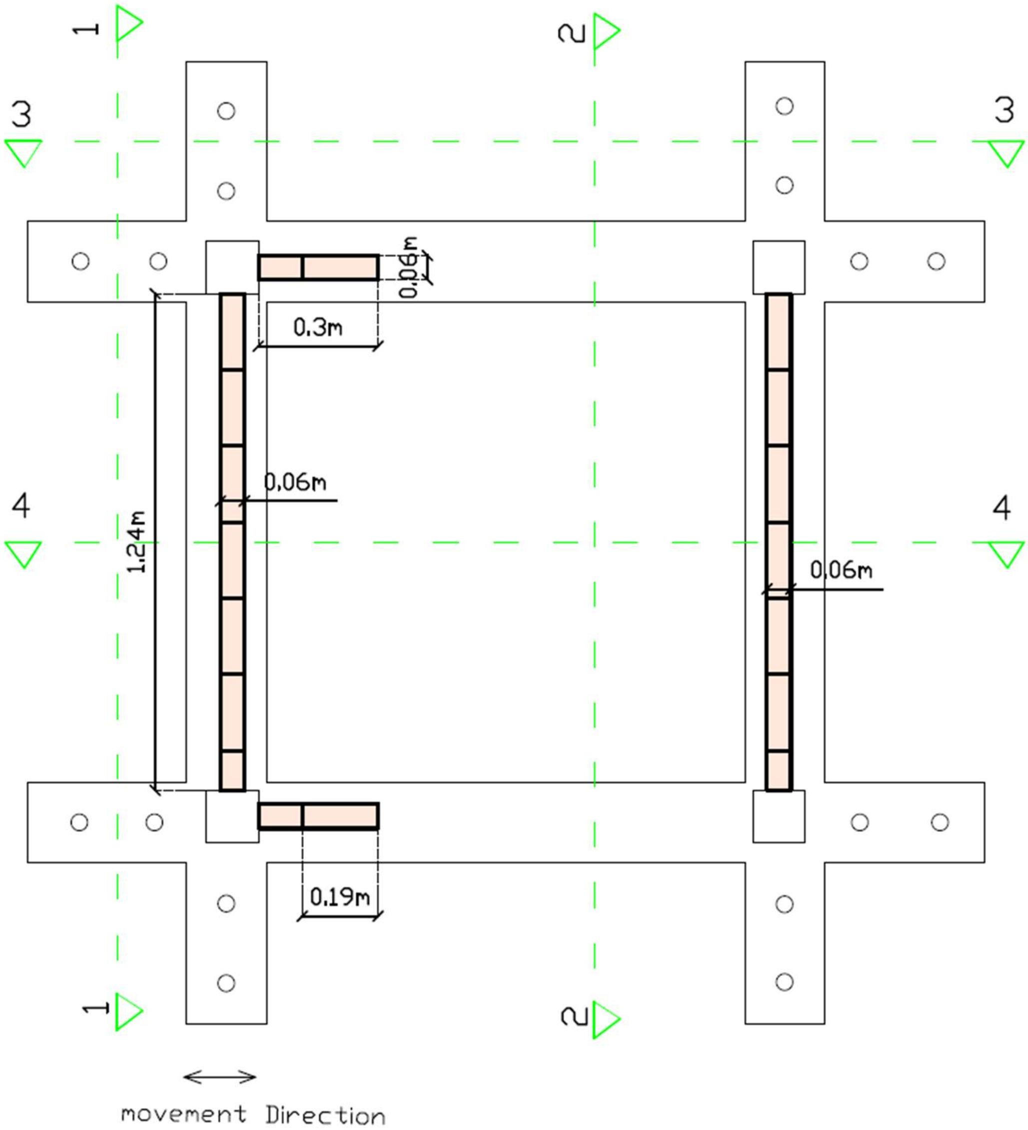

Figure 3.15 Floor plan of brick infill walls

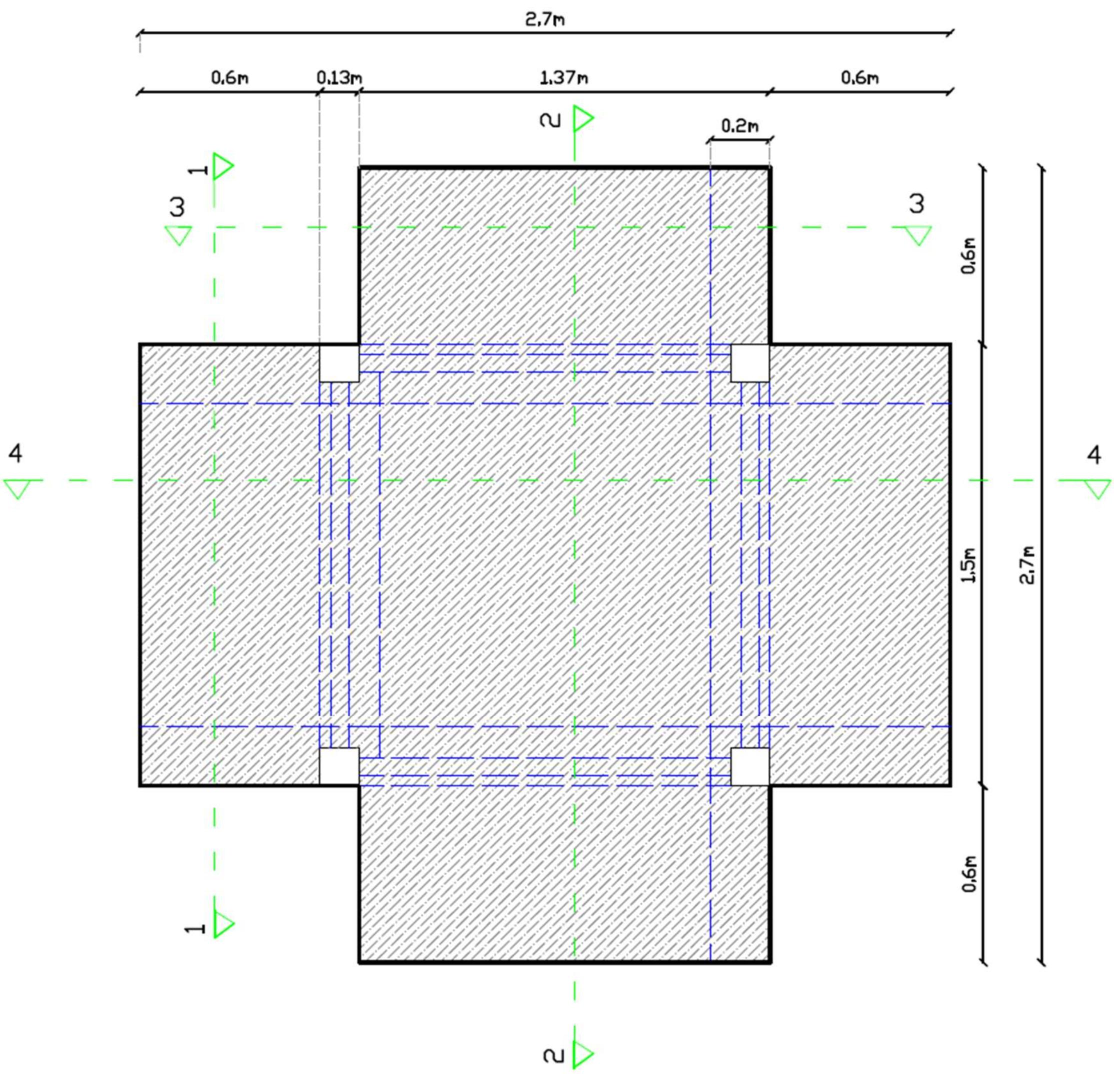

Figure 3.16 Floor plan of top slab

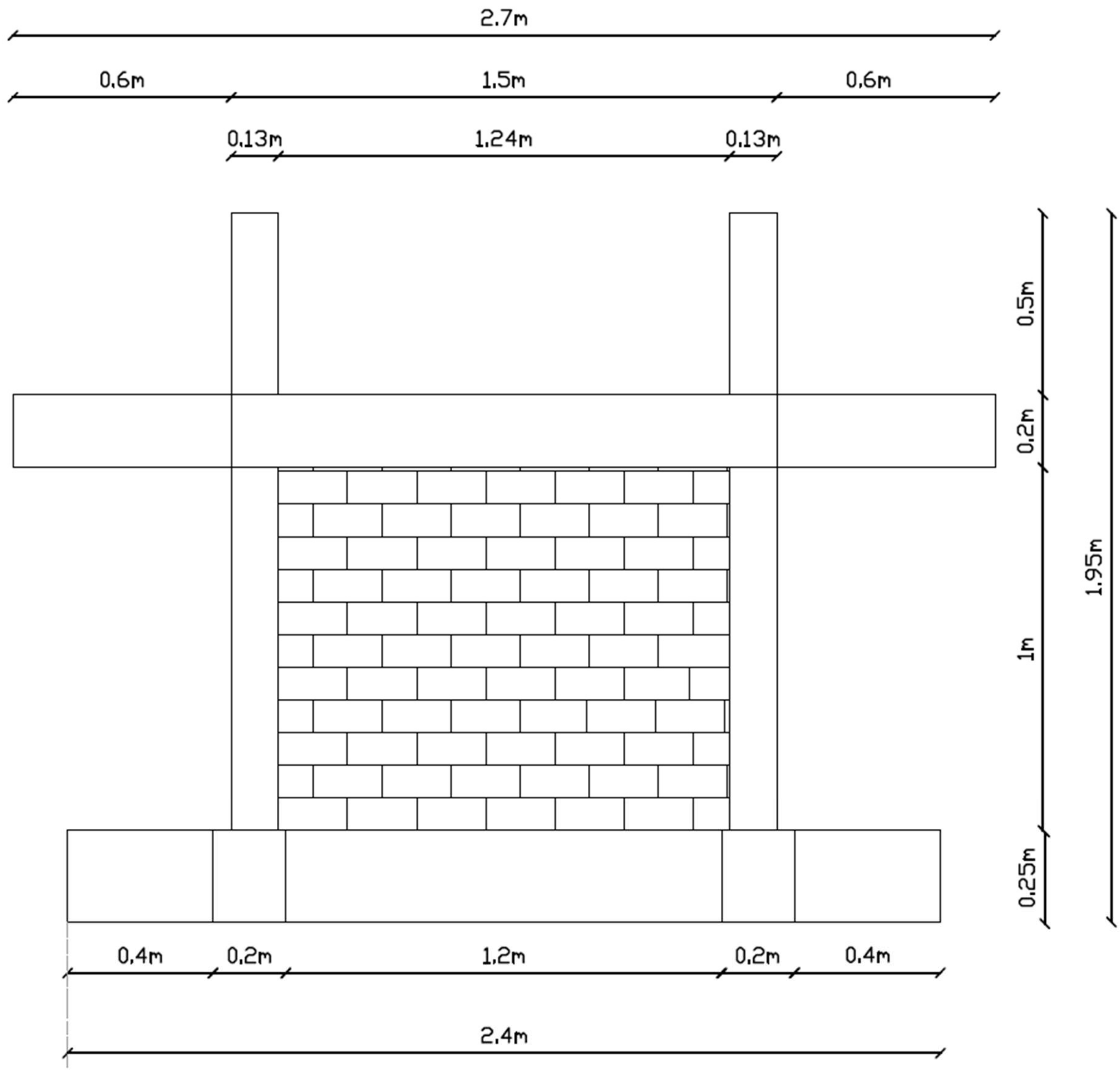

Figure 3.17 View of the structure perpendicular to the direction of loading of the seismic table

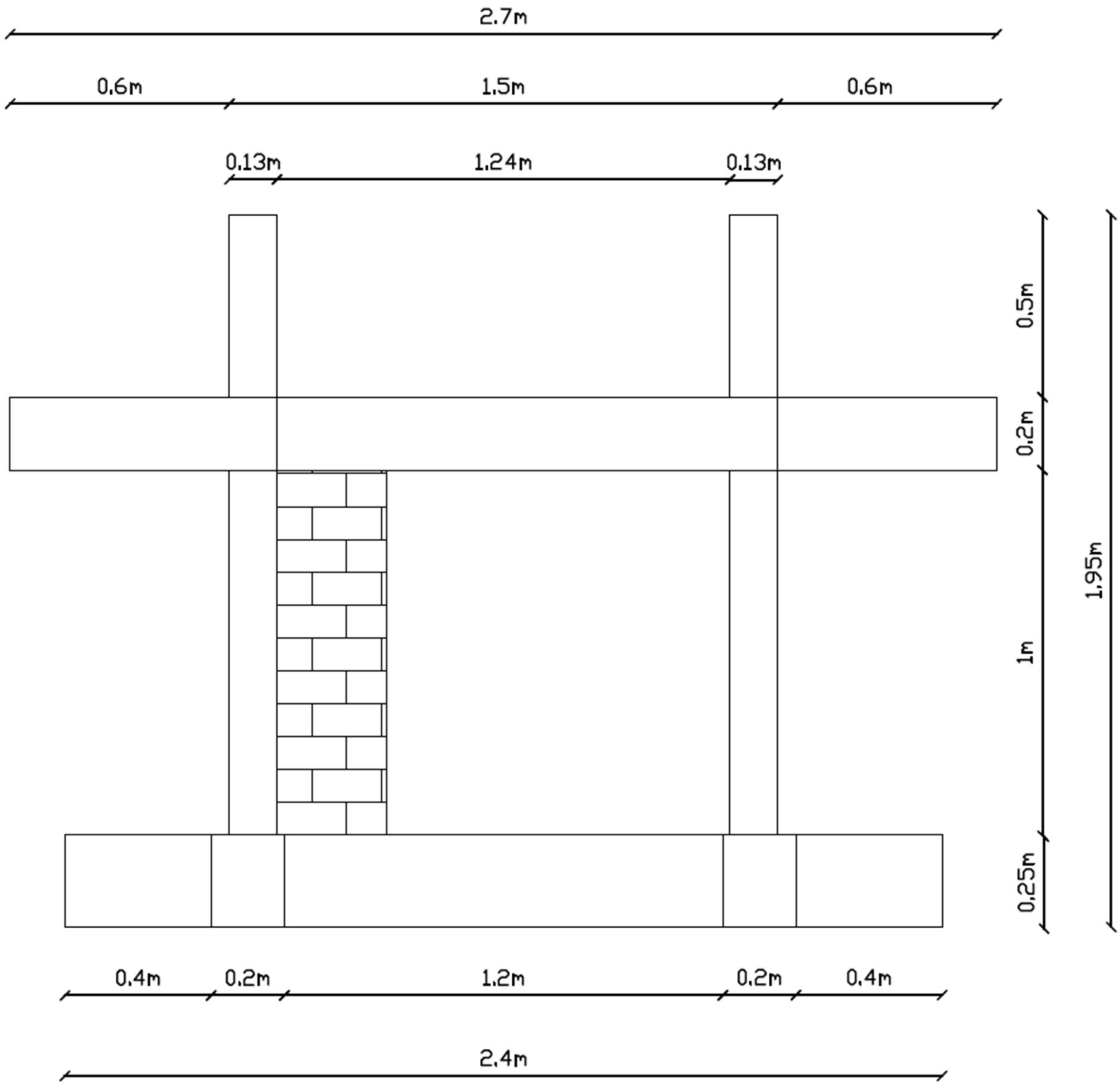

Figure 3.18 View of the structure parallel to the direction of loading of the seismic table

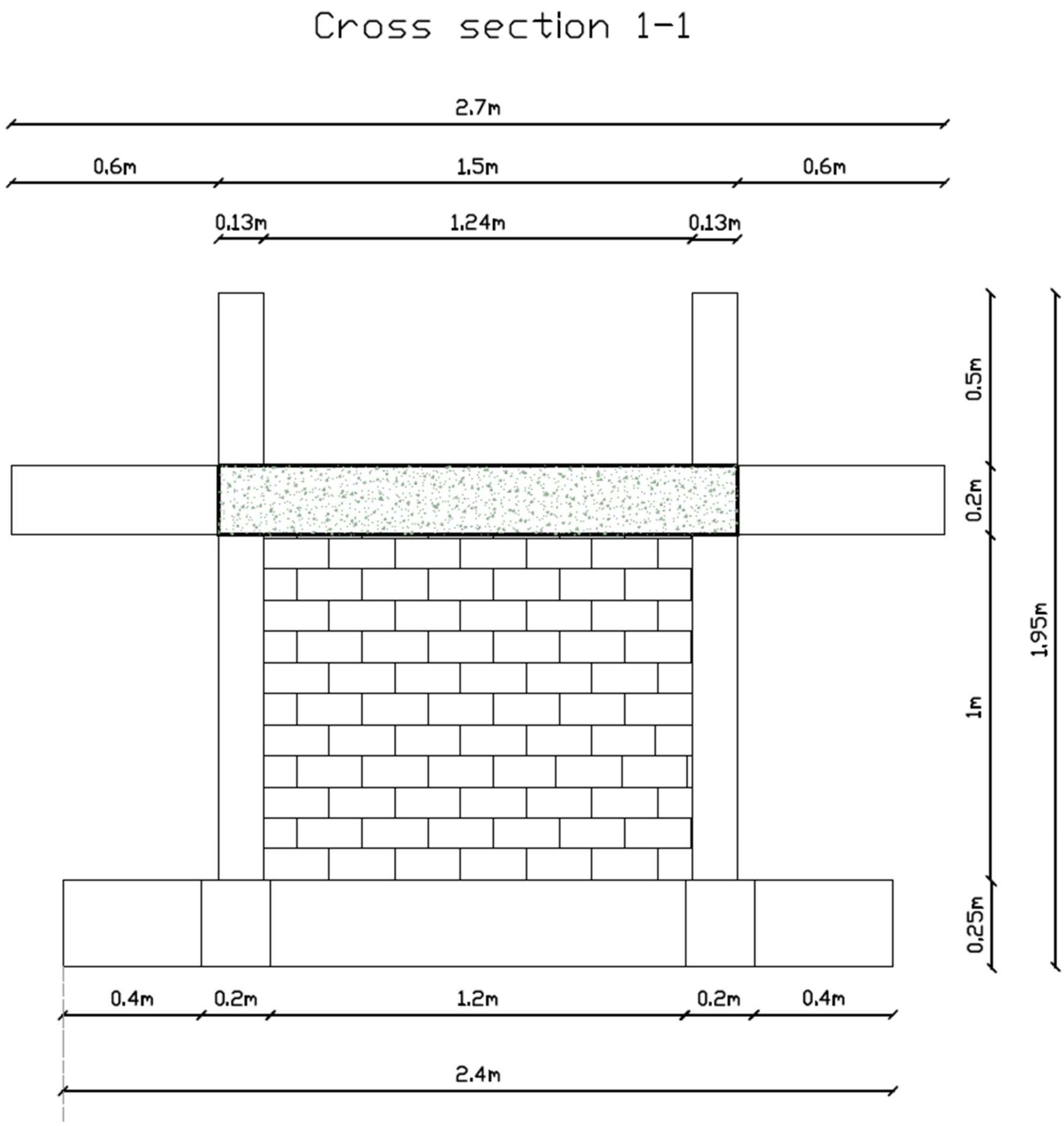

Figure 3.19 Section at the location of the external cantilever, perpendicular to the direction of movement of the seismic table

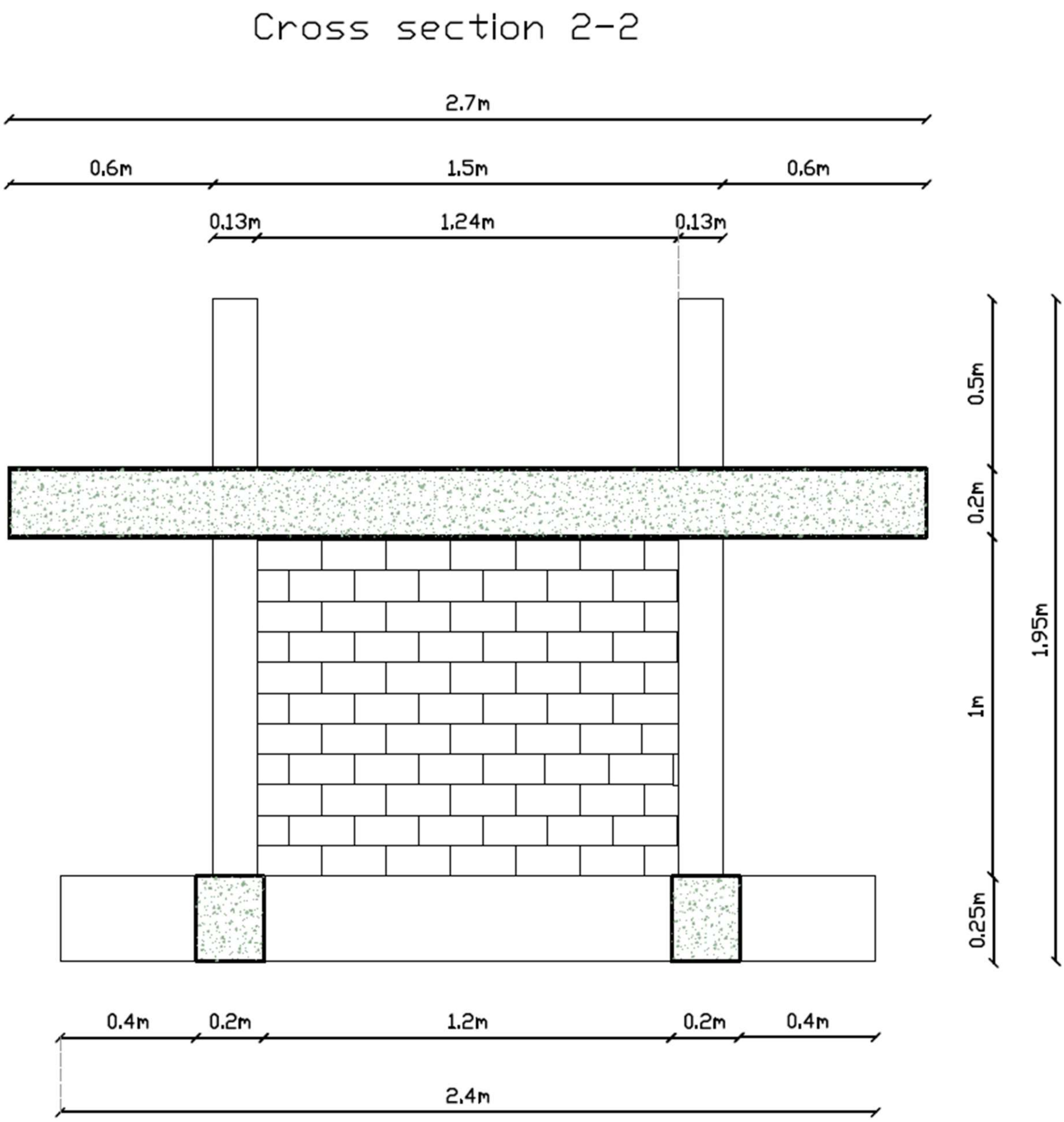

Figure 3.20 Section at the location of the internal slab, perpendicular to the direction of movement of the seismic table

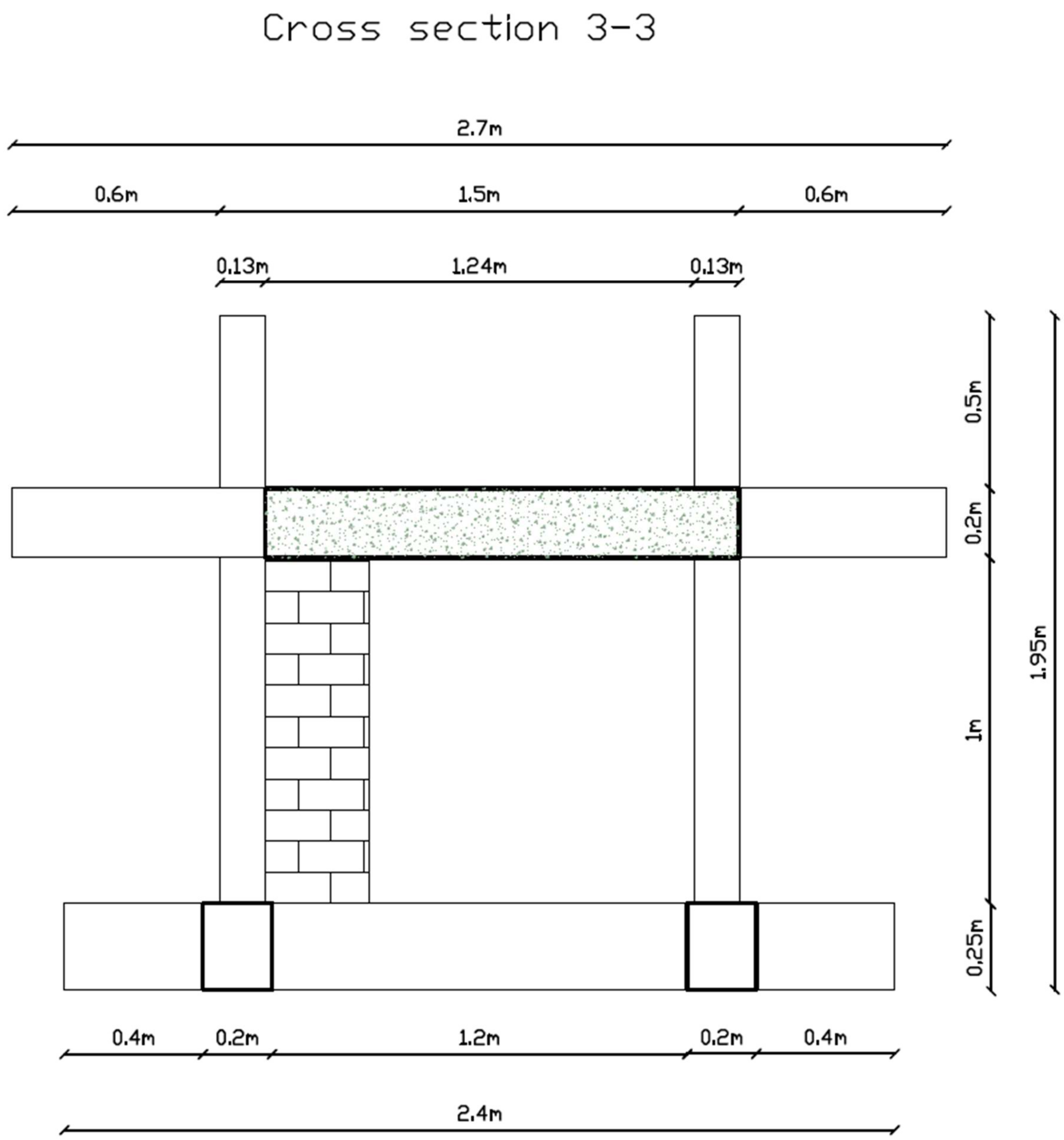

Figure 3.21 Section at the location of the external cantilever, parallel to the direction of movement of the seismic table

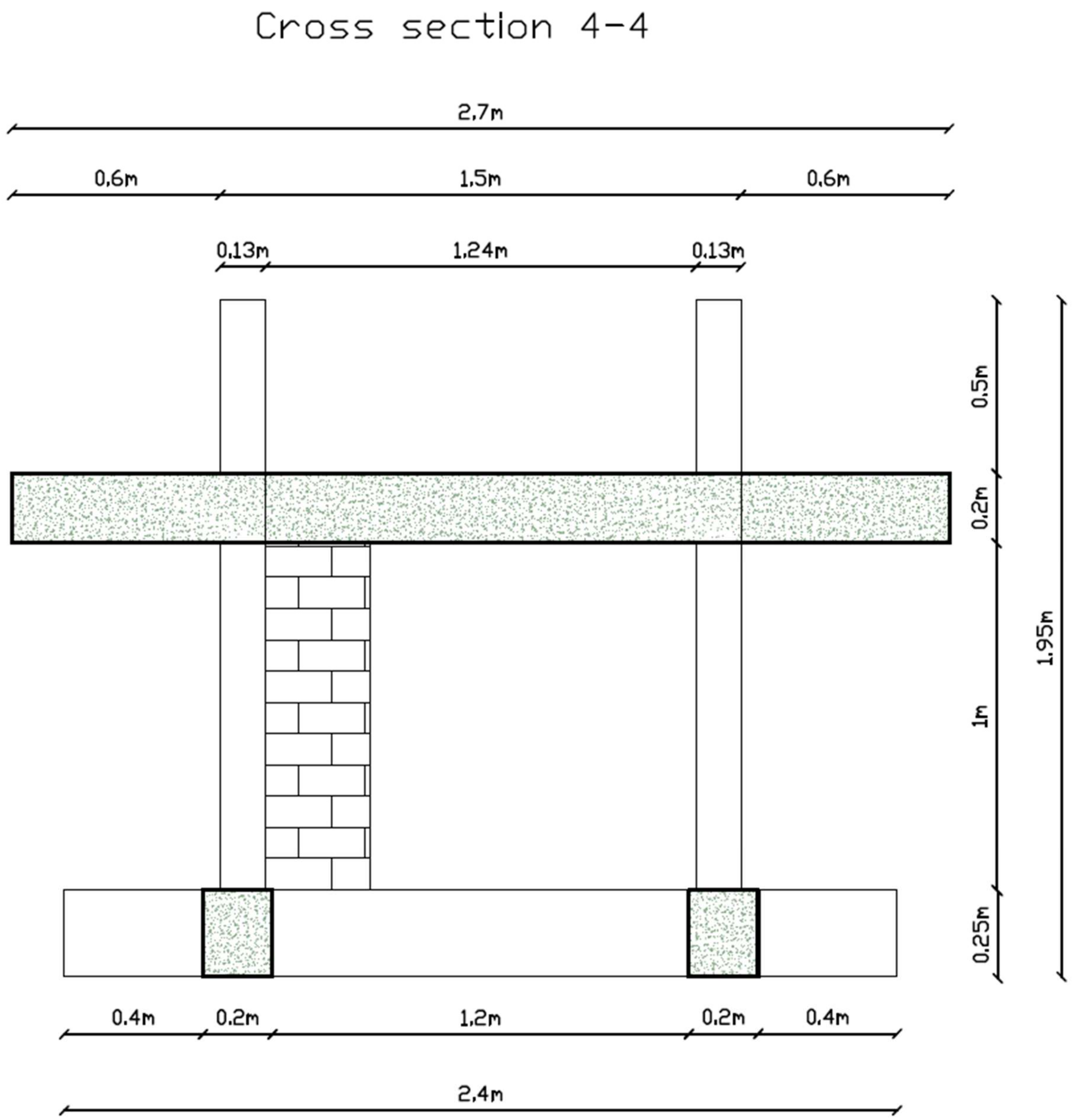

Figure 3.22 Section at the location of the internal slab, parallel to the direction of movement of the seismic table

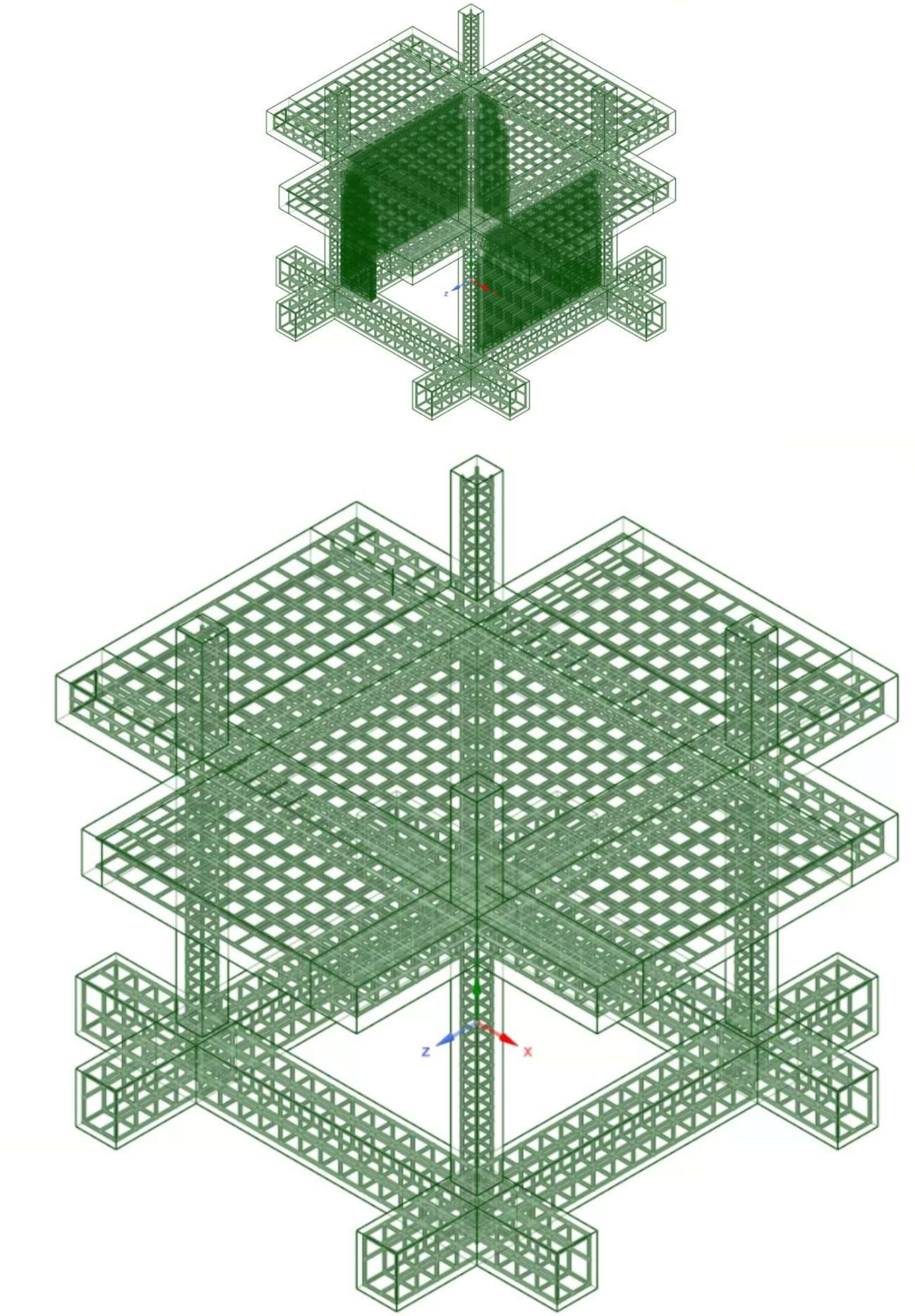

Figure 3.23 3D View of main reinforcement detailing

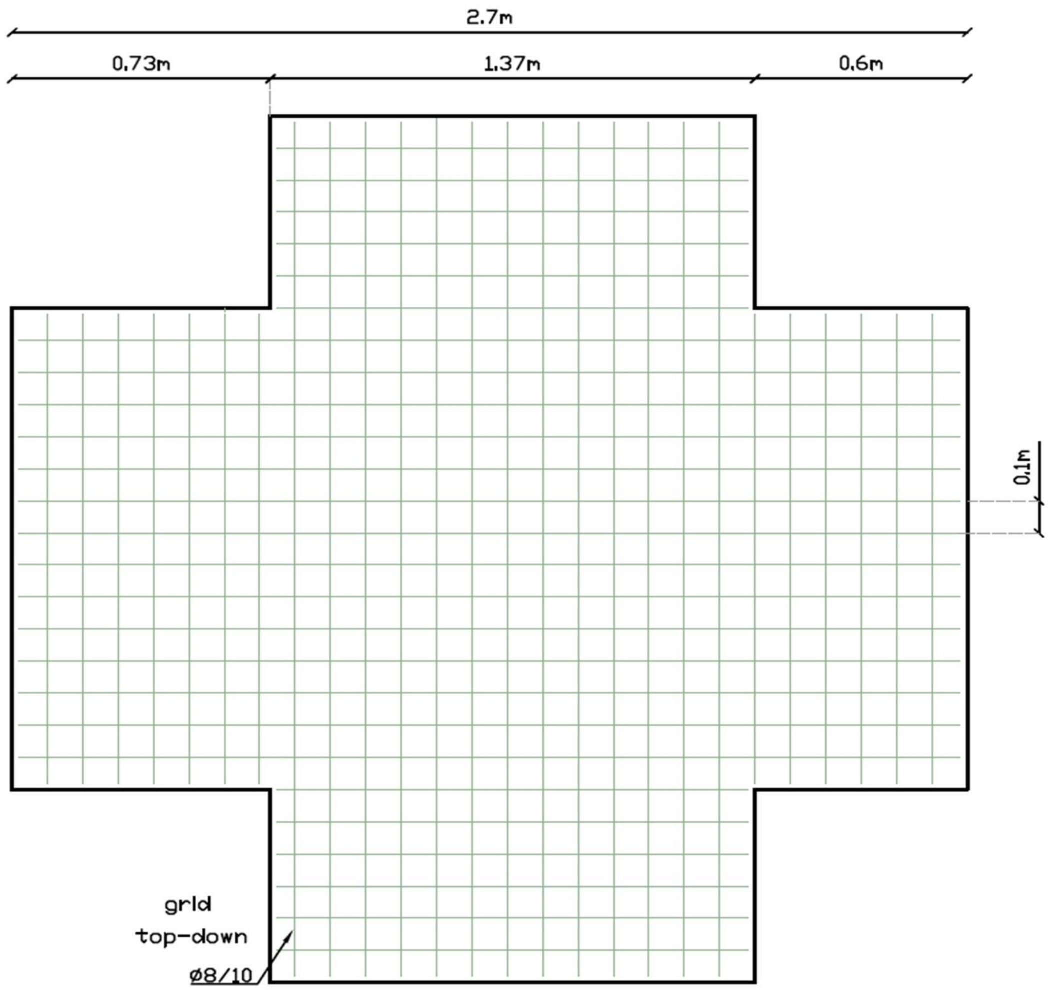

Figure 3.24 Reinforcement detailing of the top slab

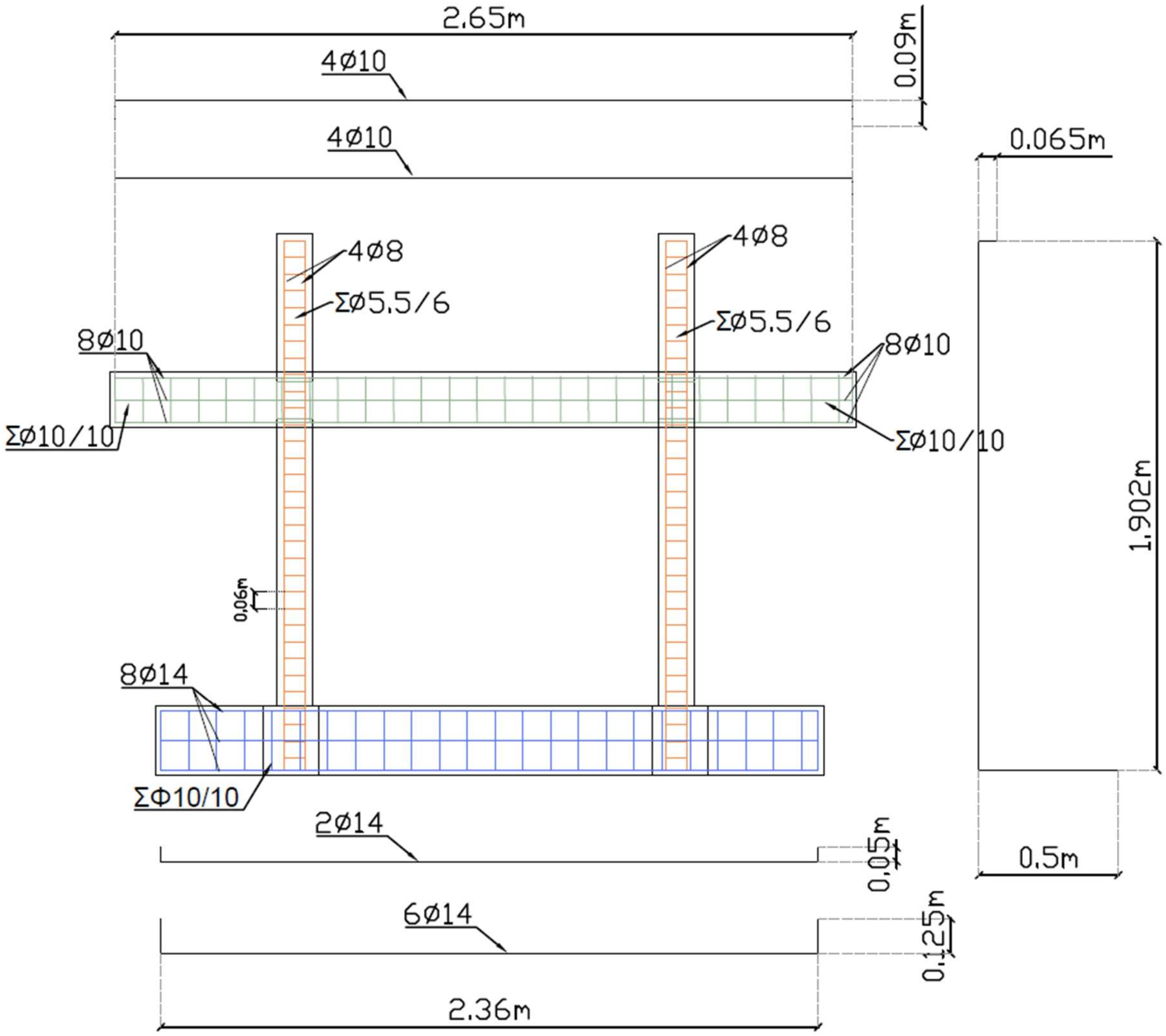

Figure 3.25 Reinforcement detailing of typical frame

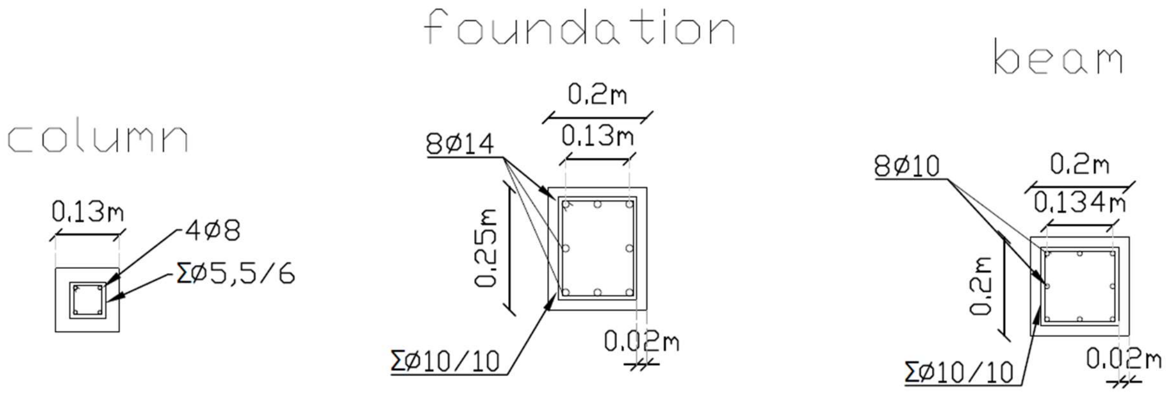

Figure 3.26 Reinforcement detailing of different member sections

3.2.2 Materials

Concrete of two categories C20/25 and C30/37 are used in the construction. The maximum aggregate diameter is 16mm. C30/37 concrete is used in the foundation beams and C20/25 concrete quality for the columns, the top slab and the top column extensions. The following materials were mixed for the C20/25 quality concrete prepared in the DUTh laboratory: cement II 32,5R, CEMI 42,5R, water and aggregates. More specifically there were used 180 kg/m3 CEM II 32,5R, 120 kg/m3 CEM I 42,5 R, water 199 kg/m3 and aggregates. The aggregates consisted of 798 kg/m3 crushed stone gravel, 350 kg/m3 crushed stone sand and 675 kg/m3 natural river sand. The total weight of aggregate for 1m3 concrete was 1822 kg (see Table 3.1). In each concreting, 12 cylindrical samples were taken to determine the concrete strength class. From the total of cylinders of each concreting, 3 were used to determine the compressive strength at 28 days. The rest of the specimens will be tested to failure to determine the mechanical characteristics of concrete on the day of the shake table testing experiments.

As for steel, two categories B500C and S220 are used in the construction. Ribbed bars of B500C steel quality are used in longitudinal bars of columns, in longitudinal bars and stirrups of the foundation beams and of top beams hidden inside the top slabs. Smooth steel of S220 quality is used for the stirrups of the columns.

Bricks for infill walls are hollow clay units by KEBE with dimensions 60/90/190 mm (width/height/length) and weight of about 1,2kg brick.

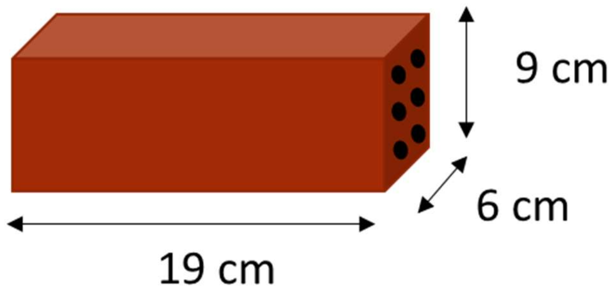

Figure 3.27 Dimensions of the brick

Table 3.1: Composition of the mix for C20/25 concrete quality

Type of materials	Type	Material proportions (kg/m^3)
cement	CEM II 32,5R	180
cement	CEM I 42,5R	120
water	network	199
aggregate	origin of aggregates	
crushed stone gravel		798
crushed stone sand		350
natural river sand		674
Total weight of aggregate for 1m3 concrete		1822

3.2.3 Reinforcements of the structure

The different reinforcements of the structure are as follows (Table 3.2): in the foundation beams, longitudinal reinforcement is 8Ø14 and stirrups Ø8/100 mm. The weight of the longitudinal reinforcement in the foundation is 99.4 kg while that of the stirrups is 32.7 kg. Longitudinal reinforcement with a weight of 15.5kg and stirrups Ø5.5/60 mm with a weight of approximately 7.5kg were placed in the columns. Also, longitudinal reinforcement 8Ø10 with a weight of 55kg and stirrups Ø10/100 mm with a weight of 45.7kg was placed in the hidden beams. Finally, an upper and lower Ø8/100 mm grid was used in the slab, with a total weight of 87,4kg.

Table 3.2: Detailed description of the rebars used and calculation of its weight

Position	Form of rebars	Rebars	Length(m)	Pieces (×4)	Total Length (m)	Weight (kg/m)	Total Weight (kg)
Foundation (beam P1-P2-P3-P4)	Longitudinal	2Ø14	2,46	2x4	19,68	1,208	23,7
		6Ø14	2,61	4x6	62,64	1,208	75,7
	Stirrups	Ø8/100	0,94	(24+20)x2	82,72	0,395	32,7
Columns (K1-K2-K3-K4)	Longitudinal	4Ø8	2,47	4x4	39,6	0,395	15,5
	Stirrups	Ø5,5/60	0,316	32x4	63,4	0,186	11,8
Beams (D1-D2-D3-D4)	Longitudinal	8Ø100	2,94	8x4	94,08	0,617	58
	Stirrups	Ø10/100	0,84	(27+23)x2	171,36	0,617	51,8
Slab	top						
	Ø8/100				110,6	0,395	43,7
	bottom						
	Ø8/100				110,6	0,395	43,7
	Slab free edge loop reinforcement of shape U Ø8/100				84,8	0,395	33,5
Sum							400

The total mass of the steel reinforcement, including special anchorage and montage detailing reached 450kg.

3.2.4 Total volume of the structure

In the tables below, the total volume of the foundation beam is initially calculated (concrete and steel). The total volume of the columns below and above the slab is then calculated. Finally, the total volume of the slab and of the hidden beams is calculated. The volumes are added and the final volume of the construction is obtained equal to 1.68 m^3.

Table 3.3: Calculation of the total volume of the structure

	Dimensions			
Foundation beam		4 segments		
	Length (m)	Height (m)	Width (m)	Volume 1 (m^3)
	2,4	0,25	0,2	0,12
	Total			0,48
Common area of foundation beam				
		4 segments		
	Length (m)	Height (m)	Width (m)	Volume 2 (m^3)
	0,2	0,25	0,2	0,01
	Total			0,04
Total volume of foundation beams			Volume 1 – volume 2	0,44
Columns		4 segments		
	Length (m)	Height (m)	Width (m)	Volume 3 (m^3)
	1	0,13	0,13	0,0169
	Total			0,0676
Columns over slab		4 segments		
	Length (m)	Height (m)	Width (m)	Volume 4 (m^3)
	0,5	0,13	0,13	0,00845
	Total			0,0338
Total volume of columns			Volume 3 + volume 4	0,1014

Table 3.4: Calculation of the total volume of the structure

	Dimensions			
Slab – hidden beams	**Length (m)**	**Height/thickness (m)**	**Width (m)**	**Volume 5 (m^3)**
	2,7	0,2	2,7	1,458
Subtraction of corner areas of the slabs	Length (m)	Height (m)	Width (m)	Volume 6 (m^3)
	0,2	0,6	0,6	0,144
	0,2	0,6	0,73	0,1752
Total slab volume			Volume 5 – volume 6	1,1388

Total volume of structure is 1,68 m^3

3.2.5 Specific weight of concrete

The structure consists of four subsequent stages of concrete casting: the foundation beams, the columns below the slab, the slab diaphragm and the columns above the slab. Concrete cylinders were cast for each different stage. The precise dimensions of these specimens are measured. Then, the specific weight of concrete is calculated in table 3.5, 3.6.

Table 3.5: Calculation of specific weight of columns and slab

Columns and slab, beams	*d* (mm)	*L* (mm)	*W* (kg)	*B* (kN)	γ_c (kN/m^3)	γ_{cm}(kN/m^3)
Cyl_1	149	290	11,26	0,110	21,84	22,14
Cyl_2	148	294	11,50	0,113	22,31	
Cyl_3	148	290	11,33	0,111	22,28	

Table 3.6: Calculation of specific weight of foundation

Foundation (beam)	d (mm)	L (mm)	W (kg)	B (kN)	γ_c (kN/m^3)	γ_{cm}(kN/m^3)
Cyl_1	149	296	11,69	0,115	22,22	22,45
Cyl_2	148	295	11,77	0,115	22,75	
Cyl_3	149	295	11,74	0,115	22,39	

The corresponding mass of concrete and reinforcement per different construction stage is shown in the tables 3.7, 3.8.

Table 3.7: Calculation of the total mass of concrete of the structure

Concrete	V (m^3)	γ_{cm}	mass x 101,97 (kg)
Foundation beams	0,44	22,45	1007,46
Columns under slab	0,0676	22,14	152,96
Columns over slab	0,0338	22,14	76,48
Slab	1,1388	22,14	2570,66

Table 3.8: Calculation of total mass of the reinforcement of structure

Steel	Longitudinal bar total weight (kg)	Stirrups total weight (kg)	Sum (kg)
Foundation beam	99,44	32,7	132,11
Beams	58,05	51,8	109.85
Columns under slab	11,5	8,1	19,6
Column over slab	4.0	3.7	7.7
	grid (top and bottom)		
Slab	121		121

Therefore, the total mass of concrete and reinforcement at each level is as follows. For the foundation beam 1139,6 kg, For the columns below the slab 172.6 kg. For the 4 brick walls the mass is 200kg. For the slab and hidden beams, total mass is 2691,7 kg. For the columns above the slab 84,1 kg. So, the total mass of the whole structure is 4288 kg. Finally, the mass at the slab level is the mass of the slab and the mass of the columns above the slab and the half mass of the columns below the slab and of the infill walls, equal to 2962,1 kg.

3.2.6 Mechanical volumetric ratio of confining reinforcement of the columns and Eurocode requirements

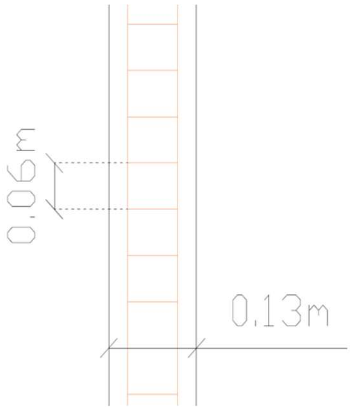

Figure 3.28. Detailing of the stirrups of the column

The materials used to calculate the coefficient α are concrete C20 and steel S220. The coefficient of efficiency α for the confinement is given by the relation α = αn * αs. The individual factors are calculated below.

$$v_d = \frac{NEd}{Ac \times fxd} = \frac{1{,}35 \times 20}{0{,}0169 \times \left(\frac{20}{1{,}50}\right) \times 1000} = 0{,}12 \quad \text{(rough estimate)}$$

$d_1 = c_{nom} + Øw + ØL/2 = 28 + 5,5 + (8/2) = 37,5$ mm

$b_i = \frac{b-2\ x\ d1}{n-1} = \frac{130-2\ x\ 37,5}{2-1} = 55$ mm

$d = h_c - d1 = 130 - 37,5 = 92,5$ mm

$h_o = 130 - 56 - 8 = 66$ mm

$b_o = h_o = 66$ mm

$A_o = h_o\ x\ b_o = 66\ x\ 66 = 4356$ mm2

$Ac = 0,13\ x\ 0,13 = 0,0169\ m^2 = 16900$ mm2

$α_s = (1 \frac{s}{2\ x\ bo})\ x\ (1 \frac{s}{2\ x\ ho}) = (1 - \frac{60}{2\ x\ 66})\ x\ (1 - \frac{60}{2\ x\ 66}) = 0,30$

$α_n = 1 - \frac{\sum_{i=1}^{n} bi^{\wedge}2}{6\ x\ bo\ x\ ho} = 1 - \frac{2\ x\ (2\ x\ 55^2)}{6\ x\ 4356} = 1 - 0,46 \rightarrow αn = 0,54$

$α = α_n\ x\ α_s = 0,54\ x\ 0,30 = 0,162$

$ω_{wd} = \frac{Lσυ \quad (cm)xAsw(cm2)x\ fywd}{s\ x\ Ao\ x\ fcd}$

$h - c_{nom} - c_{nom} - \frac{Φw}{2} - \frac{Φw}{2} = ho = bo = 66$ mm

$ω_{wd} = \frac{Lσυνδ\ (cm)xAsw(cm2)x\ fywd}{s\ x\ Ao\ x\ fcd} = \frac{(6.6\ x\ 4)x\ 0,237\ x\ (\frac{220}{1.15})}{6\ x\ 43,56\ x\ (\frac{20}{1.50})} = 0.343$

$α\ x\ ω_{wd} = 0,162\ x\ 0,343 = 0,0556$

minimum required $α\ x\ ω_{wd} = 30\ μφ\ x\ vd\ x\ εsy,d\ x\ (bc/bo) - 0,035 = 30\ x\ 6,8\ x\ 0,12\ x\ (\frac{220}{1,15\ x\ 200000})\ x\ (130/66) - 0,035 = 0,0112$

minimum required ω_{wd} = 0,0112/0.162 = 0.069, ≥0.08. Provided confinement seems adequate based on Eurocode requirements because of the low value of assumed axial load.

Where:

h_c: is the gross cross – sectional depth

ho: is the depth of confined core (to the centerline of the hoops)

bc: is the gross cross – sectional width

bo: is the width of confined core (to the centerline of the hoops)

vd: is the normalized design axial force

$\omega_{wd} = \frac{\text{volume of confining hoops}}{\text{volume of concrete core}} \times \frac{\text{fyd}}{\text{fcd}}$

n: total number of longitudinal bars laterally engaged by hoops or cross ties on perimeter of coloumn section

n =2 at the direction of b and

n = 2 at the direction of h

α = is the confinement effectiveness factor, equal αn x as

For rectangular cross sections:

$\alpha_s = (1 - \frac{s}{2 \, x \, bo}) \times (1 - \frac{s}{2 \, x \, ho})$

$\alpha_n = 1 - \frac{\sum_{i=1}^{n} bi^{\wedge}2}{6 \, x \, bo \, x \, ho}$

3.2.7 Instrumentation

The instrumentation includes 12 uniaxial accelerometers (ACC) located at the 4 positions indicated in Figure 3.29. Three accelerometers provide the three components of acceleration at each point, that is in- and out-of-plane accelerations at the center of the full infills, as well as the accelerations of the top slab and of the bottom foundation beam. Four draw wire sensors (W) measure the horizontal displacement of the foundation beams and of the top slab as depicted in Figure 3.30. Further, 2 draw wire sensors measure the change of distance along the 2 diagonals of the two partial infills (in-plane deformation) Figure 3.31 (total of 4 draw wire meters). Draw-wire displacement sensors measure linear displacement using a highly flexible and relatively rigid under tension, steel wire. The cable drum is attached to a sensor element which provides a displacement-proportional output signal. During construction, 16 strain gauges (S) were glued on the longitudinal reinforcement of the columns. Two strain gauges were placed on the lower side of each column and two on the upper side. Finally, 39 PZTs (P) were placed inside the concrete mass of the columns and of the top slab as indicated in Figure 4.5.

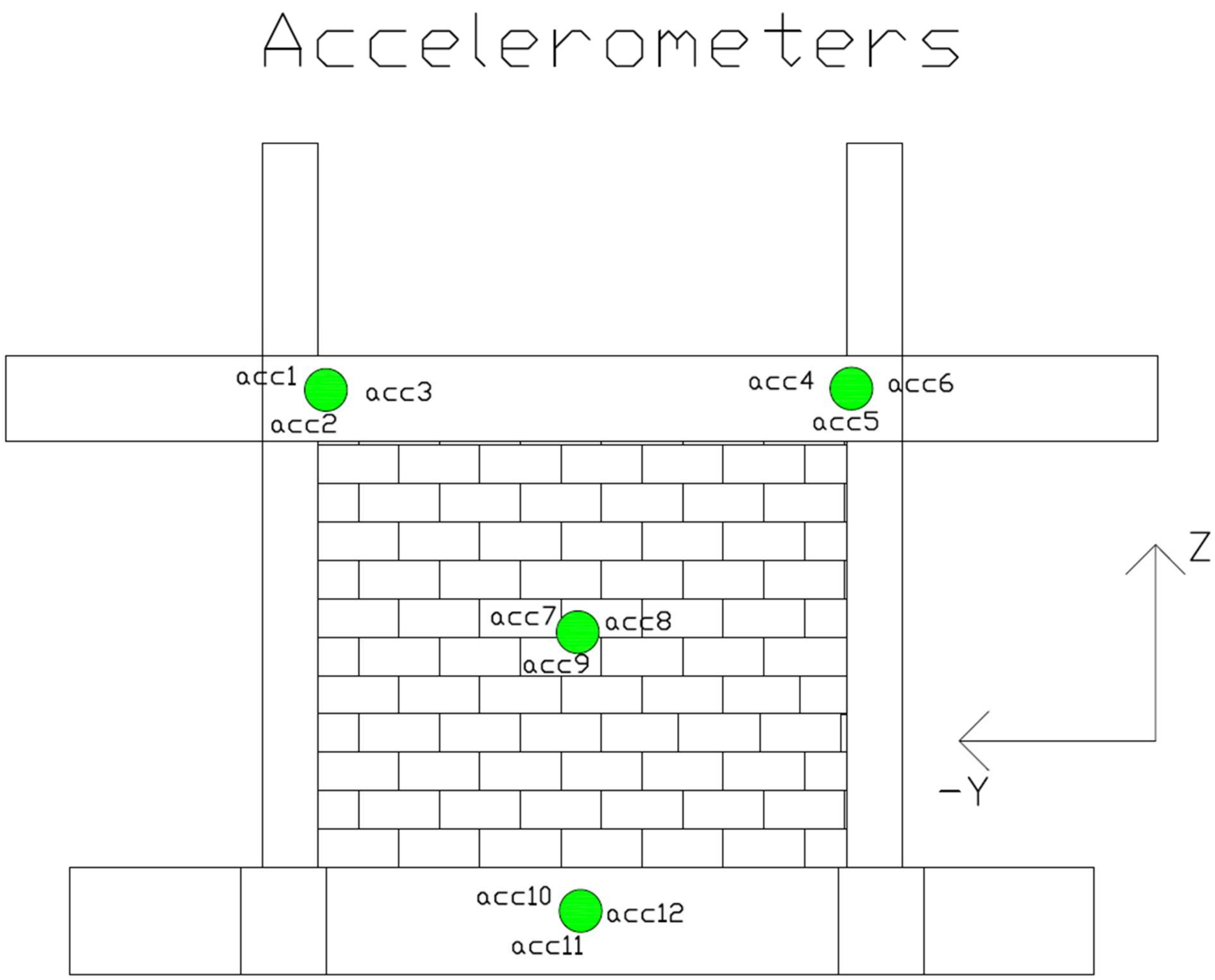

Figure 3.29 Figure 3.30 Position of accelerometers (specimen's view perpendicular to the direction of the seismic table movement)

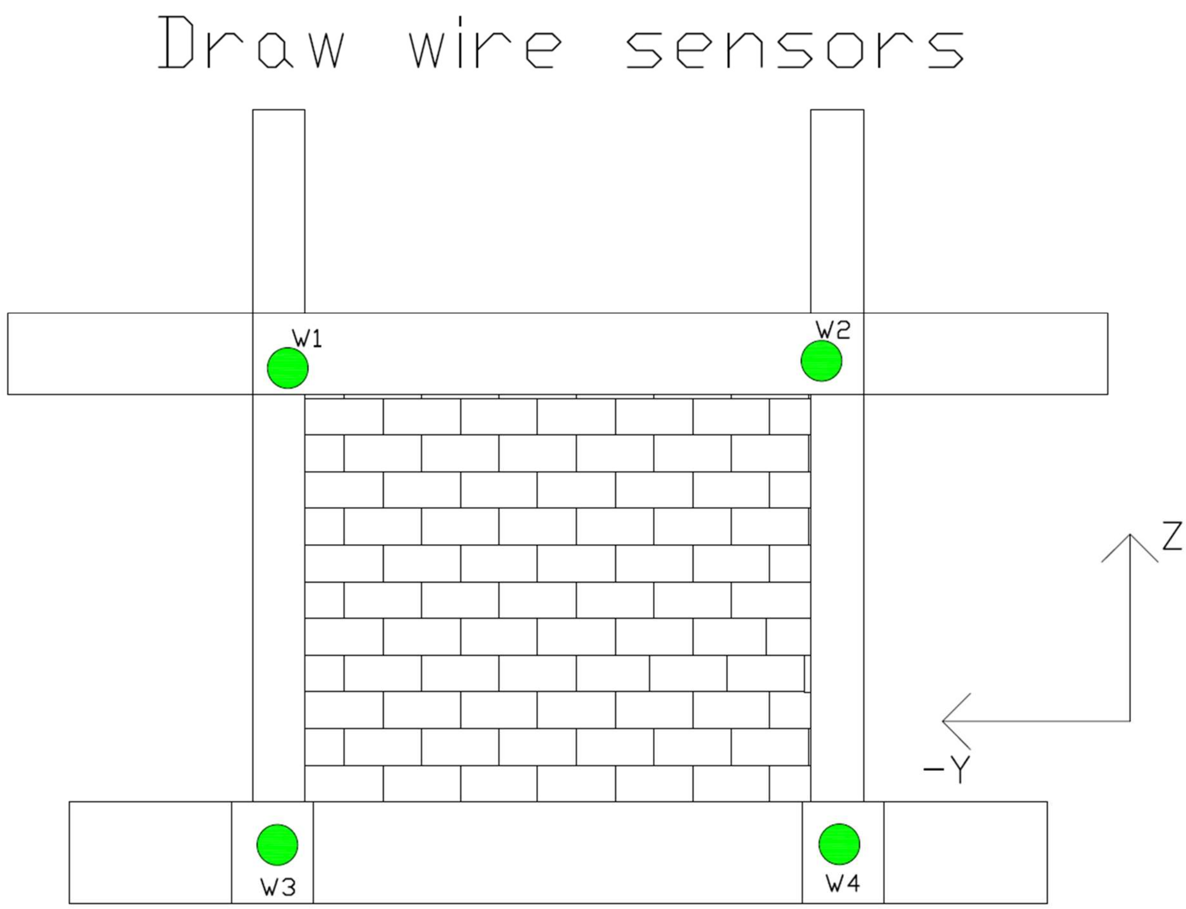

Figure 3.30 Position of the draw wire sensors on the concrete structure slab and foundation beams (specimen's view parallel to the direction of the seismic table movement)

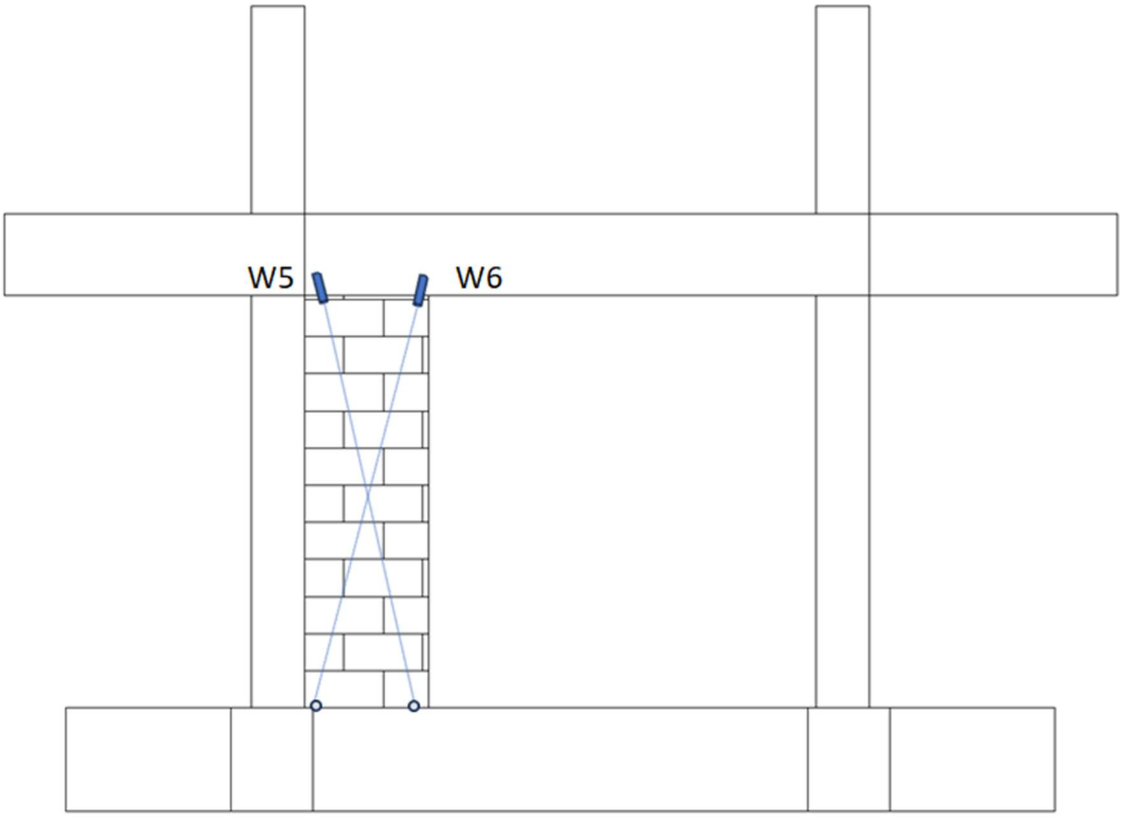

Figure 3.31 Position of the diagonal draw wire sensors, along the diagonals of the partial infil (specimen's view parallel to the direction of the seismic table movement)

Table 3.9: List of accelerometers, draw wire meters and strain gauges placed inside and on the structure

Ch No.	Channel name	Type of instrument	Measured quantity (units)	Position
1	ACC 1	Accelerometer	Acceleration (g)	On the slab, on the left corner, dir. (x)
2	ACC 2			On the slab, on the left corner, dir. (y)
3	ACC 3			On the slab, on the left corner, dir. (z)
4	ACC 4			On the slab, on the right corner, dir. (x)
5	ACC 5			On the slab, on the right corner, dir. (y)
6	ACC 6			On the slab, on the right corner, dir. (z)
7	ACC 7			On the infill, on the center, dir (x)
8	ACC 8			On the infill, on the center, dir (y)
9	ACC 9			On the infill, on the center, dir (x)
10	ACC 10			On the foundation, on the center, dir (x)
11	ACC 11			On the foundation, on the center, dir (y)
12	ACC 12			On the foundation, on the center, dir (z)
13	W 1	Draw wire sensors	Length (mm)	On the slab, on the left side
14	W 2			On the slab, on the right side
15	W 3			On the foundation, on the left side
16	W 4			On the foundation, on the right side
17	W 5			along the partial masonry infill diagonal
18	W 6			along the partial masonry infill diagonal
19	W 7			along the partial masonry infill diagonal
20	W 8			along the partial masonry infill diagonal
21	S1	Strain gauges	Strain	In the longitudinal reinforcement, on the underside
22	S2			
23	S3			
24	S4			
25	S5			
26	S6			
27	S7			
28	S8			
29	S9			In the longitudinal reinforcement, on the upper side
30	S10			
31	S11			
32	S12			
33	S13			
34	S14			

35	S15			
36	S16			
37	S17			On the centre of partial masonry 1 along direction x
38	S18			On the centre of partial masonry 1 along direction z
39	S19			On the centre of partial masonry 2 along direction x
40	S20			On the centre of partial masonry 2 along direction z

4 DEVELOPMENT OF A SMART PZT MONITORING SYSTEM FOR THE VERTICAL FOREST (VF) STRUCTURE

Structural health monitoring for real-time condition and damage assessment in the tested VF concrete structure is performed with PZTs. Prompt damage diagnosis of seismically deficient VF buildings requires, in addition to the other common testing measurements, the monitoring and evaluation in a real-time system based on piezoelectric sensors or piezoelectric transducers (PZTs) Fig.4.1.

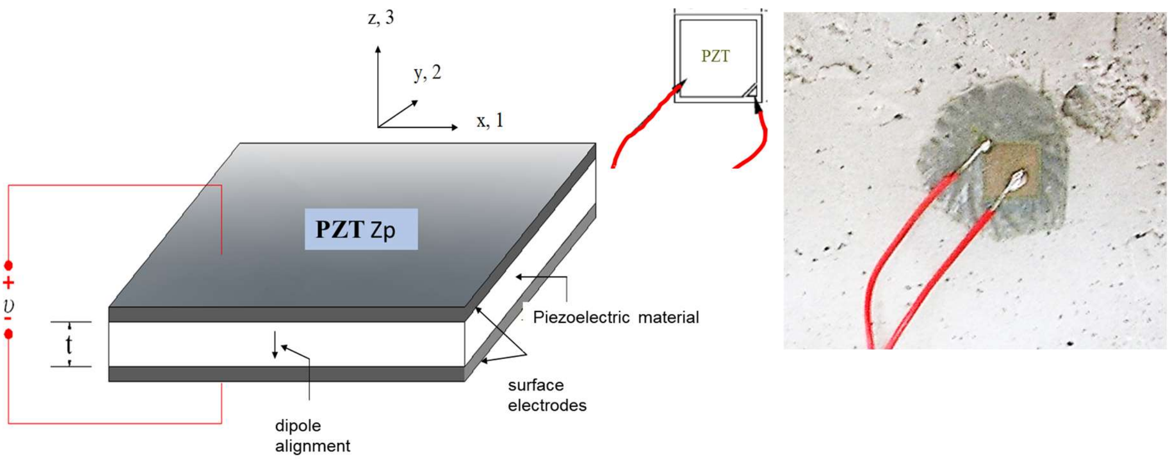

Figure 4.1 PZT connected using wires

This innovative Structural Health Monitoring (SHM) system uses sensors as a patch or an embedded-in “smart aggregate” (SAs) featuring smart properties or implements a network of piezoelectric patches to monitor the condition of the reinforced VF concrete structure. The SHM system is based on the Electro-Mechanical Impedance (EMI) sensing method utilizing the voltage signal measurements of a series PZT transducers mounted to the tested VF frames. EMI-based SHM method utilizes piezoelectric patches, which are mounted adequately to the VF structure by a robust bonding interface. Piezoelectric patches can operate as (a) actuators to vibrate the inspection area of the structure in terms of the mechanical wave with high-frequency excitations (converse piezoelectric effect) and simultaneously as (b) sensors to monitor the changes in their electrical impedance due to the impedance of the structure (direct piezoelectric effect), Fig 4.2.

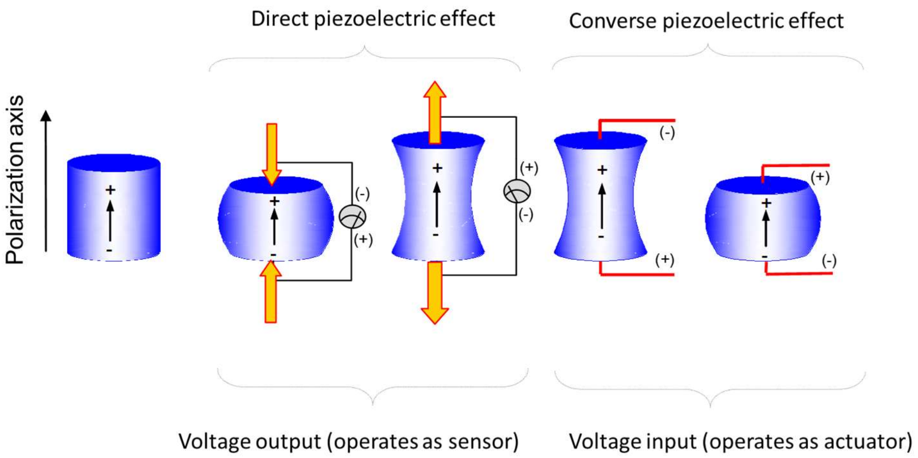

Figure 4.2 The Piezoelectric Effect: PZT as a Sensor and Actuator

PZT patches were adopted to implement the EMI measurements in real-time through a wired connection with an advanced custom-made device. The connection between the custom-made device, the PZT embedded-in SAs, and the host structure is illustrated schematically in Figure 4.3.

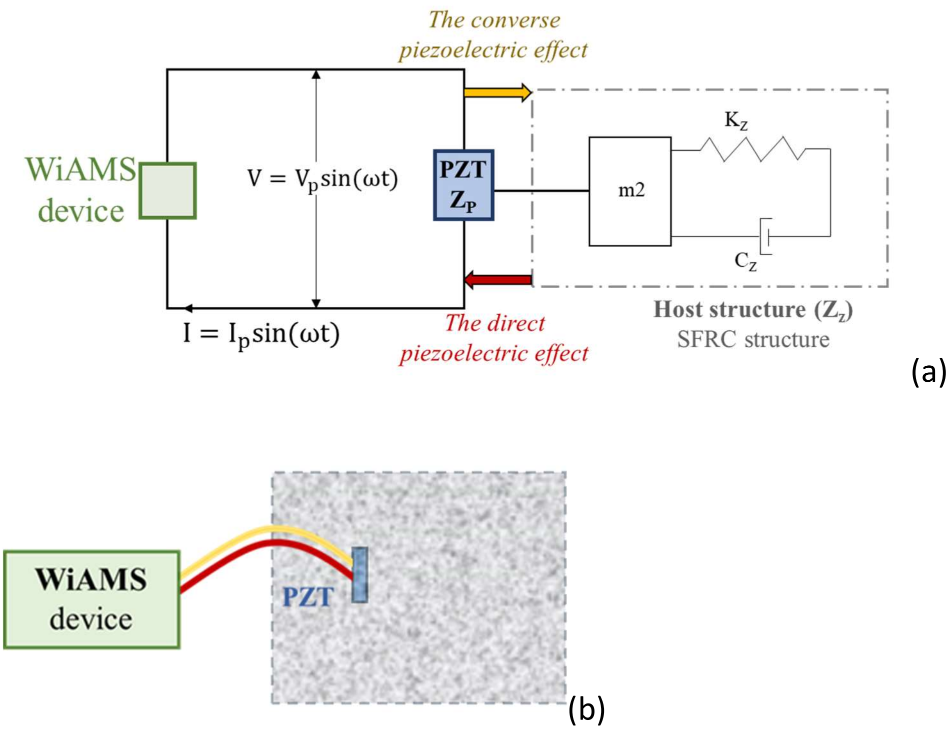

Figure 4.3 (a) Schematic of the electrical circuit in one-dimensional electromechanical impedance PZT - structure coupling system and (b) connection between the custom-made device, the embedded PZT and the host structure, circuit.

The EMI sensing method has shown promise as a technique for continuously inspecting and assessing damage in new or existing in-service infrastructures. One of the main advantages of the EMI technique is its ability to detect local damages, even in complex structures (Na et. al. 2018, Sam-Daliri Na et. al. 2018 and 2021) and composite materials (Voutetaki et. al. 2022, Naoum et. al. 2023).

Furthermore, a considerable body of literature exists on implementing the EMI-based SHM method in real-scale members, such as shear-critical RC beams (Chalioris et. al. 2015, 2016 and Voutetaki et al. 2016), RC frames (Chalioris et. al. 2020), and RC joints (Karayannis et. al. 2022) under monotonically and cyclic loading, respectively.

According to recent research, using a grid of PZT patches in areas at risk of damage can enhance the accuracy and efficiency of SHM techniques for identifying damage in reinforced concrete structures (Papadopoulos et. al. 2023).

In this step, the VF concrete structure is equipped with PZTs as embedded Sas. The SAs were placed inside the specimen mold before casting. Moreover, the embedded SAs were installed at each location orientated to the potential future flexural. The PZTs were strategically positioned to cover the longitudinal region of the beams and columns, Figure 3. Additionally, the PZTs are positioned in an array within the slab to monitor the behavior of the top part of the structure under loading, Figure 4.4.

Figure 4.4 (a) PZT patch epoxy-embedded as SAs suspended by steel wire during concrete casting to maintain the designed position in a column, (b) zoom

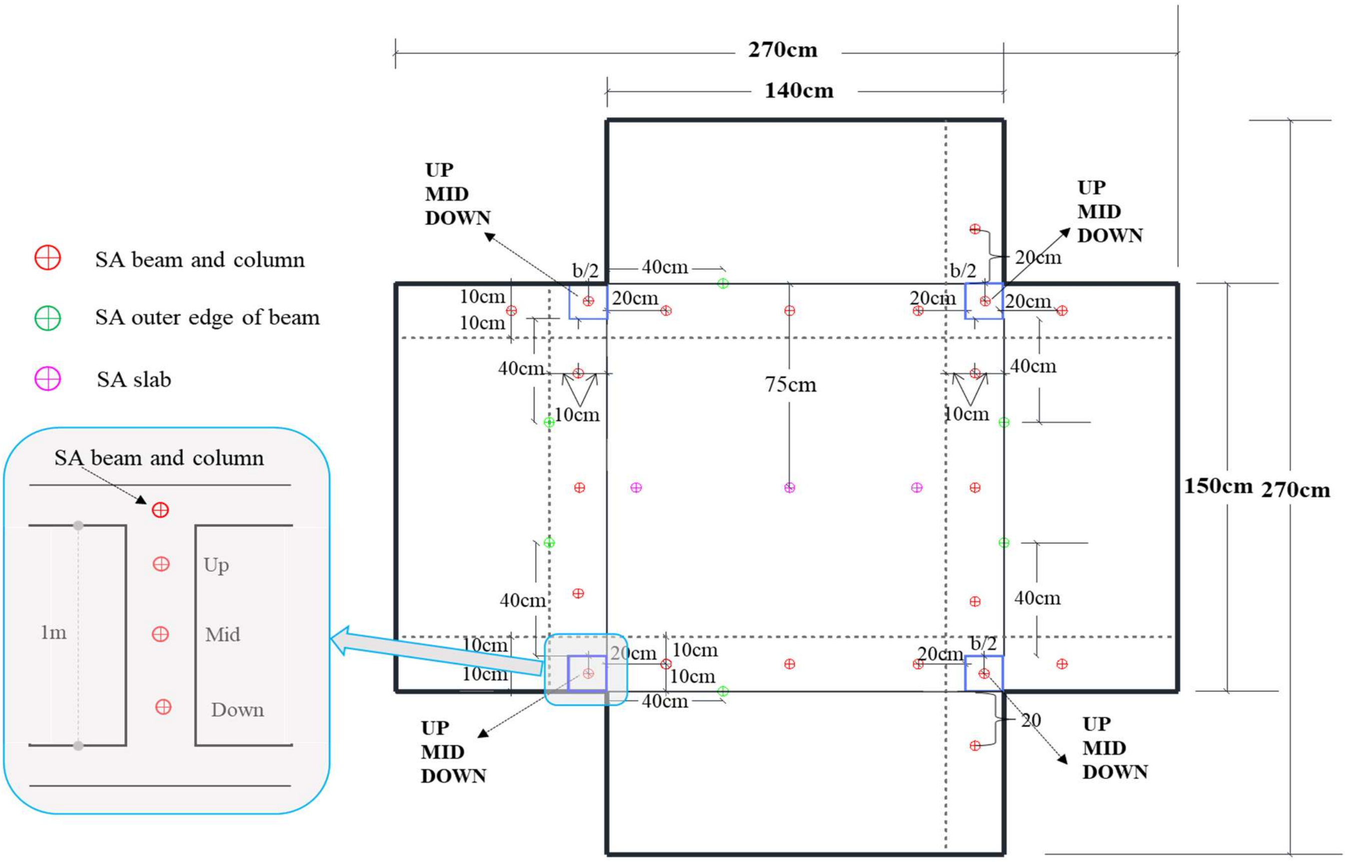

Figure 4.5 Designs and photos of detailing and instrumentation of constructed as-built 3d structure and positions of the SAs.

5 EXCITATION TIME HISTORY

The excitation executed by the shake table of DUTh will be based on the severe Thessaloniki (Volvi) earthquake of 1978. The **1978 Thessaloniki earthquake** occurred on 20 June at 23:03 local time. It was the most disastrous event in the area since the 1932 Ierissos earthquake. It was the first earthquake that hit a big city in Greece in modern times. It is estimated that 49 people died, 37 of which were living in the same block of flats in the city center that collapsed.

The building is going to be excited gradually to the damage initiation level of the as-built infill walls (up to 0.5% -0.7% lateral drift, lower than steel yielding) in plane.

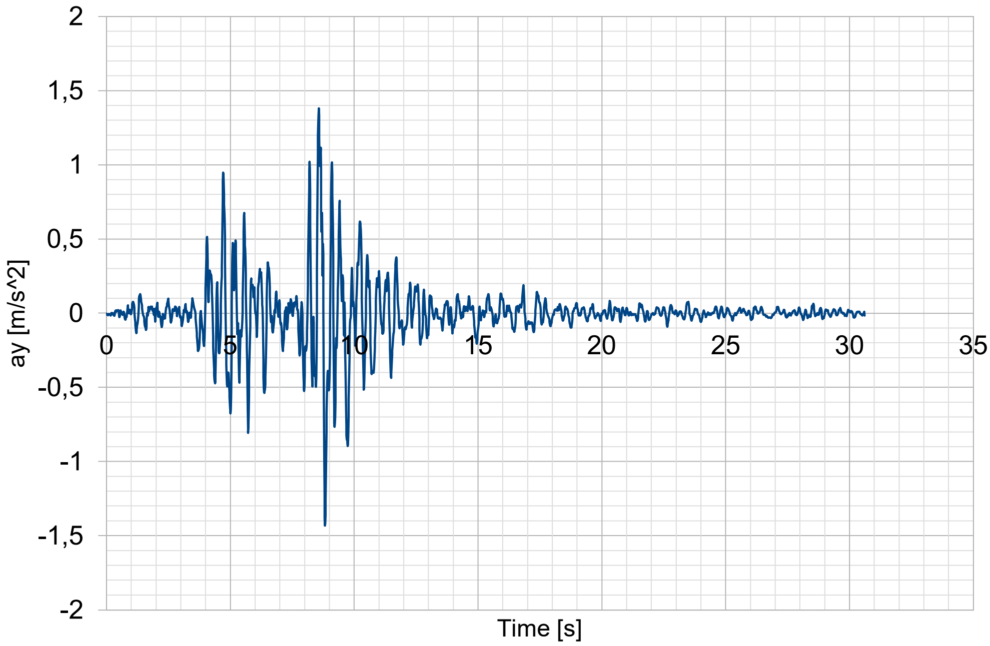

Figure 5.1 The time history executed by the DUTh seismic table, will be based on the ay component of Thessaloniki (Volvi) 1978 earthquake excitation record

6 DESIGNS AND PHOTOS OF DETAILING AND INSTRUMENTATION OF CONSTRUCTED AS-BUILT 3D STRUCTURE.

Characteristic photos of the construction phase for the RC structure are given below.

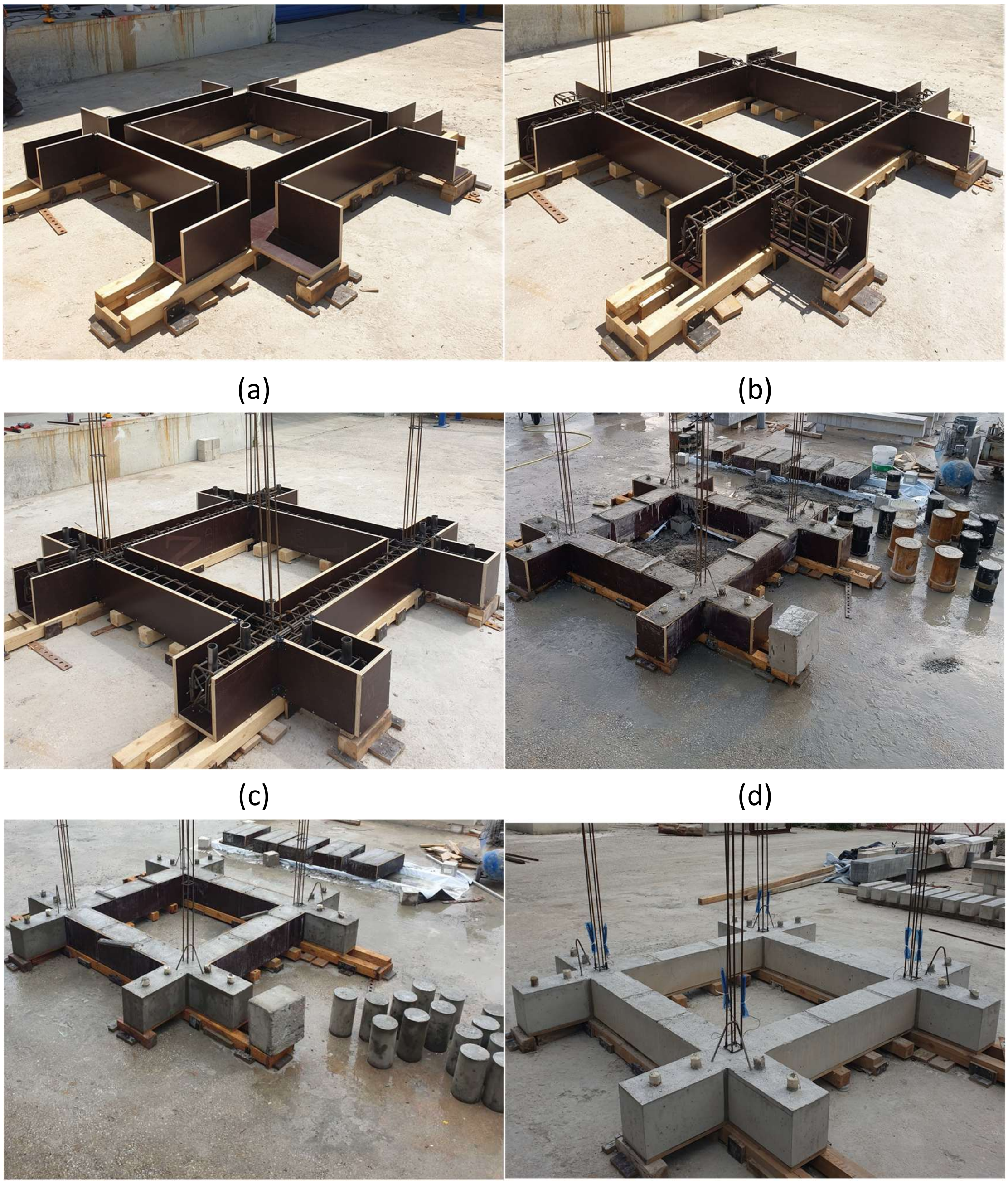

(a) (b)

(c) (d)

(e) (f)

Figure 6.1 Construction of the foundation of the specimen: (a) formwork construction, (b) installation of foundation beam reinforcement, (c) installation of longitudinal reinforcement for columns and pipes to create connection holes (for attachment to the seismic table), (d) concrete casting, (e) partial removal of the formwork, and (f) specimen's base after concrete hardening and complete formwork removal.

(a) (b) (c)

Figure 6.2 Column's reinforcement configuration: (a) and (b) longitudinal and transverse reinforcement, and (c) reinforcement detailing.

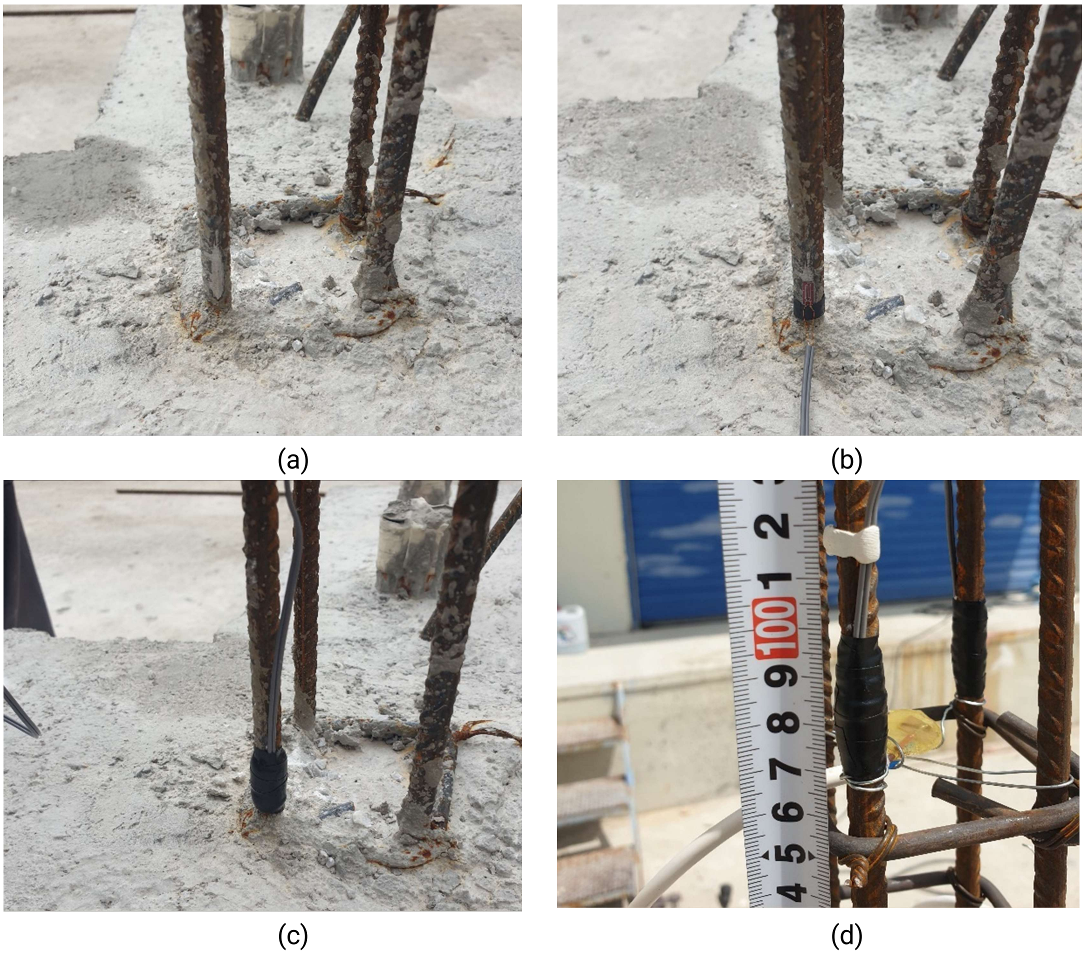

Figure 6.3 Installation of strain gauges on the longitudinal bars of the column: (a) local grinding of the bar, (b) attachment of the strain gauge, (c) protection of the strain gauge, at the base of the column, and (d) detailed positioning of strain gauges in the upper part of the column.

(a)

(b)

(c)

Figure 6.4 Construction of the specimen's columns: (a) formwork construction, (b) concrete casting, and (c) columns after concrete hardening and formwork removal.

(a) (b)

(c) (d)

Figure 6.5 On-site concrete production for column construction: (a) placement of aggregates, (b) addition of cement, (c) addition of water to the mixture, and (d) concrete after thorough mixing.

Figure 6.6 Construction of the specimen's slab: (a) scaffolding and slab formwork construction, (b) reinforcement layout, (c) detail of the slab's hidden beam reinforcement zone and lower reinforcement, PZT sensor position (d) reinforcement and formwork setup, (e) concrete casting, and (f) curing with wet burlap.

(a) (b)

Figure 6.7 Construction of infill masonry: (a) intermediate stage of masonry construction and (b) final form.

(a) (b)

Figure 6.8 Construction of columns above the slab: (a) longitudinal and transverse reinforcement configuration, and (b) formwork construction and concrete casting.

Figure 6.9 Full structure with embedded strain gauge and PZT sensors.

Figure 6.10 Panoramic view of the experimental setup (Seismic Table, Specimen, Measuring Equipment, Recording Equipment).

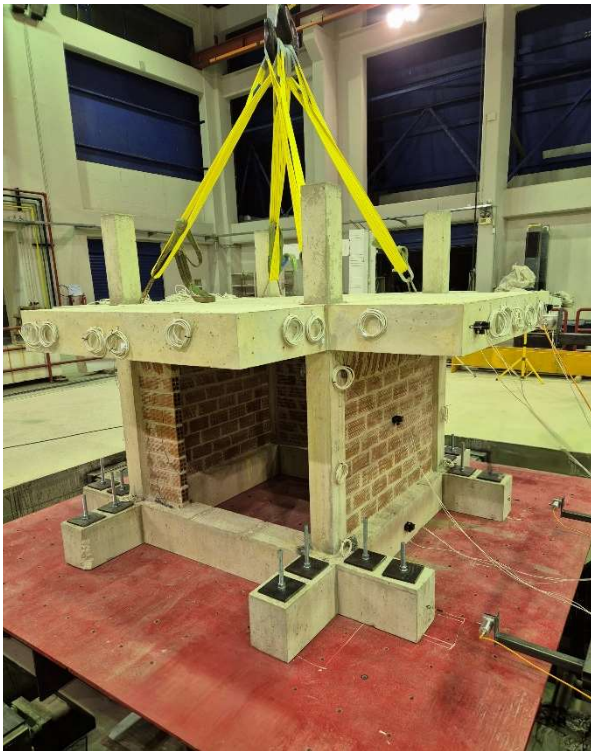

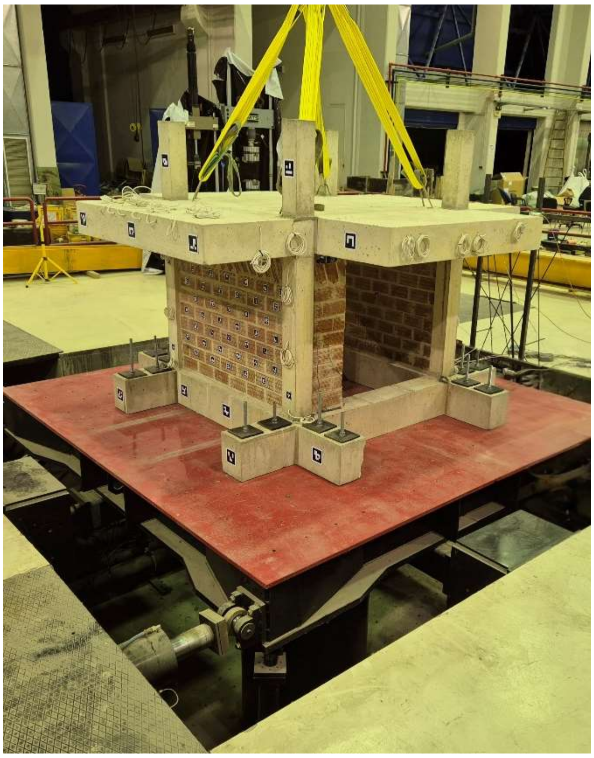

(a) (b)

(c) (d)

Figure 6.113D view of the specimen: (a), (b), (c) and (d) the different views of the test specimen and setup.

(a)

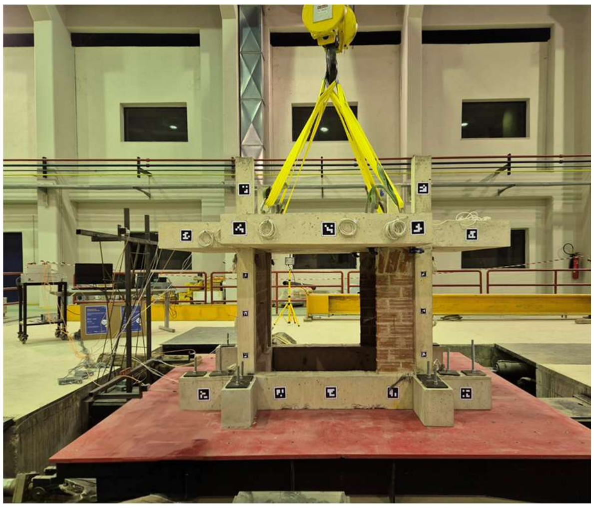

(b)

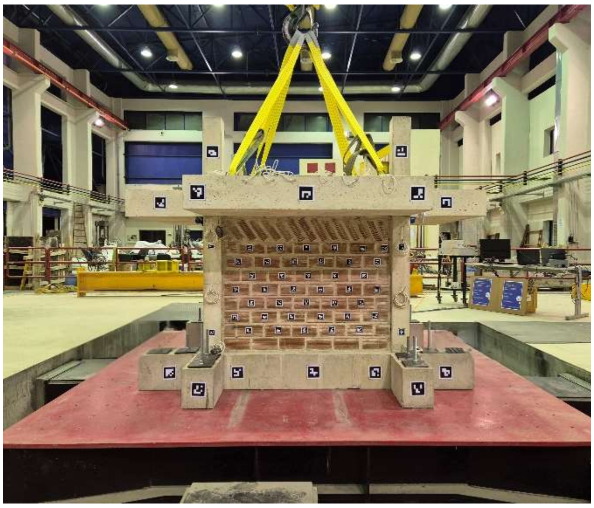

(c)

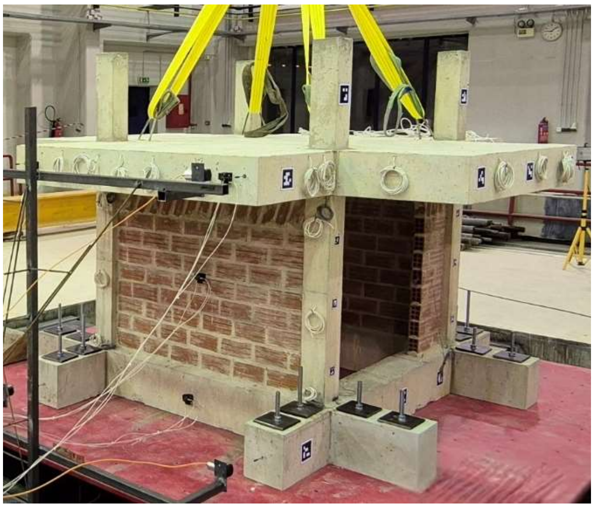

(d)

Figure 6.12 Views of the test specimen and experimental setup: (a) and (b) parallel to the movement of the seismic table (c) and (d) perpendicular to the movement of the seismic table.

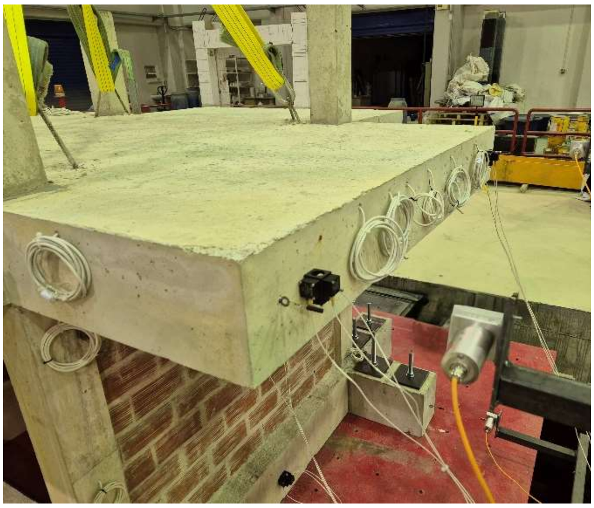
(a)


(b)


(c)

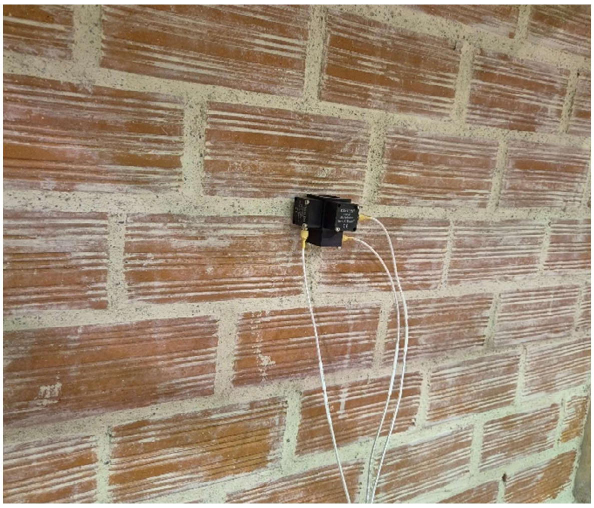
(d)

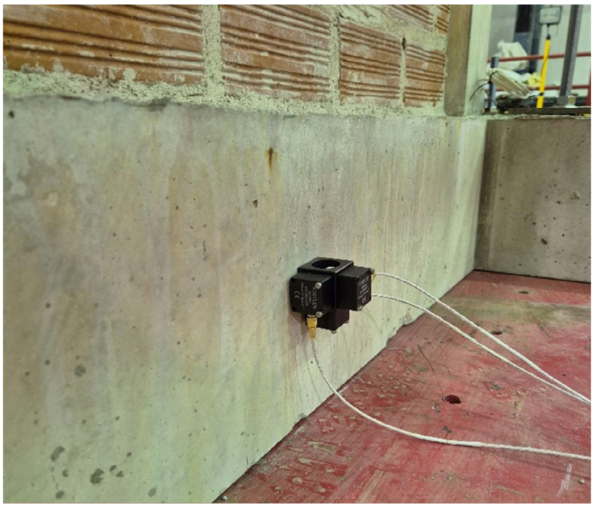
(e)

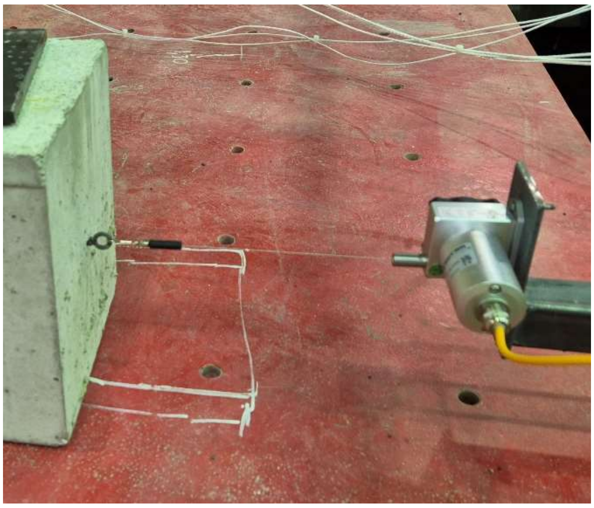
(f)

Figure 613 Instrumentation of the specimen on the side perpendicular to the direction of movement of the seismic table: (a) draw wire sensors and accelerometers on the upper slab, (b) accelerometers in the middle of the masonry and in the middle of the tie beams, (c) draw wire sensors and accelerometers on the tie beam, (d) and (e) detail of accelerometers and (f) detail of draw wire sensors.

(a)

(b)

(c)

Figure 6.14Instrumentation of masonry parallel to the direction of movement of the seismic table: (a) draw wire sensors in x-type setup and strain gauges attached in the center, (b) detail of draw wire sensors and (c) strain gauges detail.

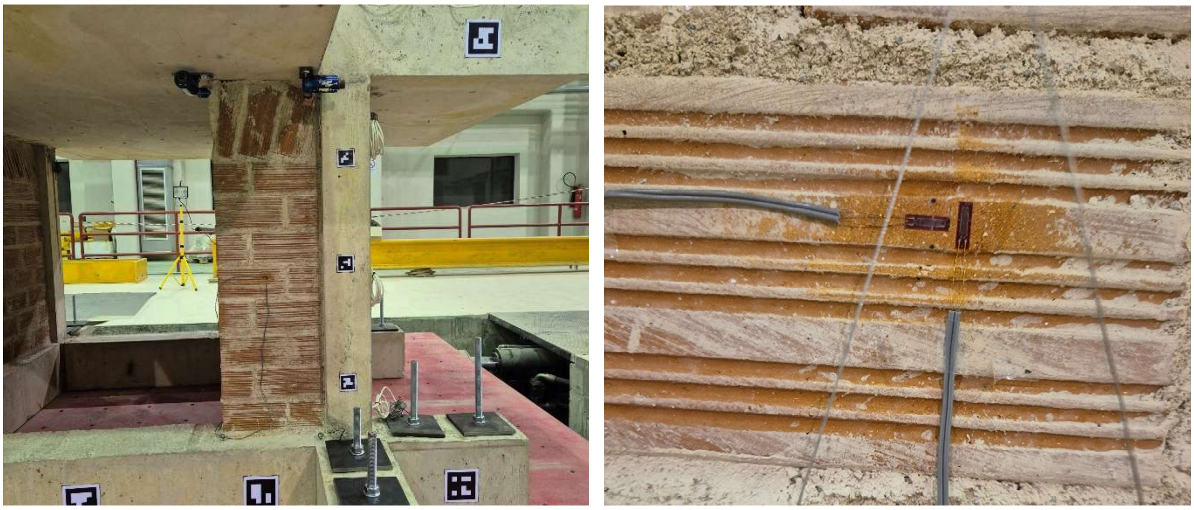

(a) (b)

Figure 6.15 Instrumentation of masonry parallel to the direction of movement of the seismic table: (a) draw wire sensors in x-type setup, optical recording marks and strain gauges attached in the center, and (b) strain gauges detail.

Figure 6.16 Instrumentation on the side transverse to the direction of movement of the seismic table with optical recording marks.

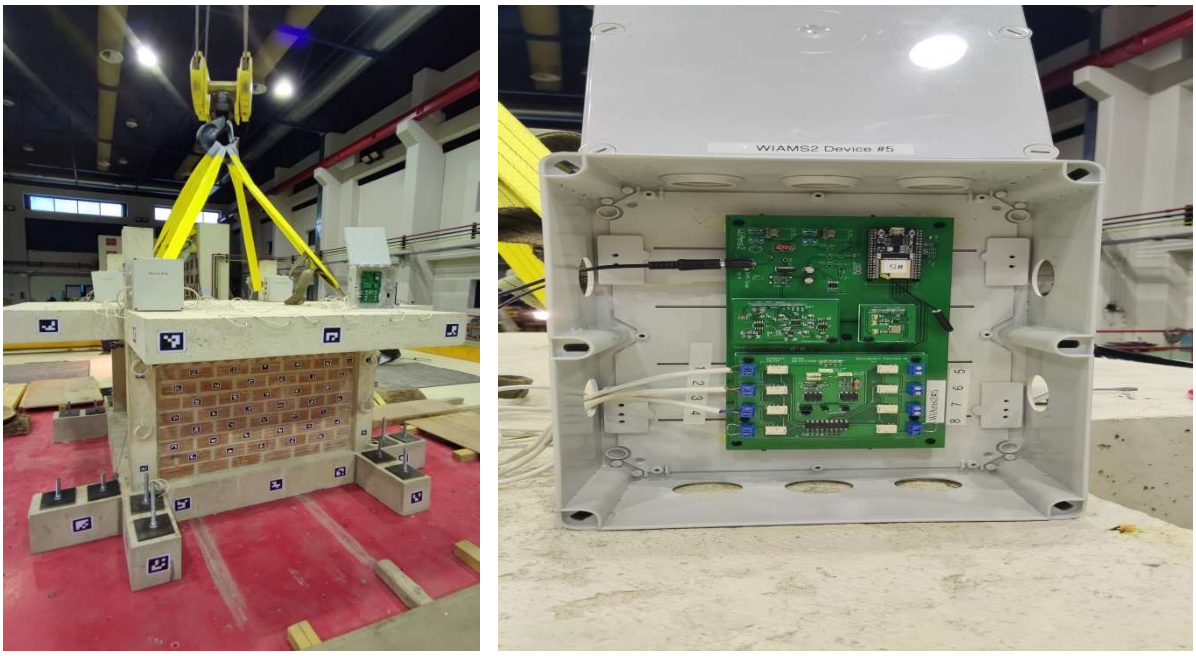

(a) (b)

Figure 6.17 Response and damage recording system with piezoelectric sensors: (a) display of the PZT system on the specimen and (b) PZT sensor data collection unit

(a) (b)

Figure 6.18 Experimental setup: (a) Specimen on the seismic table, recording system and data collection system (b) Data collection system.

7 CONCLUSIONS

This report presents in detail the designs and photos of detailing and instrumentation of constructed as-built 3d structure within the framework of workpackage of the experimental dynamic assessment of physical model structure towards holistic renovation. The building is one-bay, one-storey, consisting of a slab, four columns, four foundation beams and four brick infill walls. It is scaled down to the capacity of the seismic table of DUTh of 8tons payload and 8tnm overturning moment. It refers to old generation design codes for reinforced concrete buildings with deficient column detailing and low strength brick wall infills with low strength brick-joint mortar. The instrumentation of the structure involves advanced embedded a) innovative PZT sensors inside the concrete mass (columns, slab, and beams hidden in the slabs) as well as b) strain gauges, glued on the longitudinal bars of the four columns. Further, 3d accelerometers are attached on the slab, on the foundation beam and on the infill wall subjected to out of plane dynamic excitation. Finally, draw wire displacement meters are attached on the slab, on the foundation beams and along the diagonals of the partial infill walls subjected to in-plane dynamic excitations. The dynamic excitation of the seismic table will be based on the dynamic characteristics and severity of well-known disastrous Thessaloniki (Volvi) 1978 earthquake. The constructed 3d structure will allow for extensive and in depth basic experimental research involving advanced renovations that combine deficient RC brick infilled structure and suitable Vertical Forest constructions. Further, it will favor advanced analytical basic research towards digital twin concept and advanced structural health monitoring.

8 REFERENCES

Ai D, Luo H, Wang C, Zhu H. Monitoring of the load-induced RC beam structural tension/compression stress and damage using piezoelectric transducers. Engineering Structures 2018; 154: 38–51. DOI: https://doi.org/10.1016/j.engstruct.2017.10.046.

Ai D, Luo H, Zhu H. Numerical and experimental investigation of flexural performance on prestressed concrete structures using electromechanical admittance. Mechanical Systems and Signal Processing 2019; 128: 244–265. DOI: https://doi.org/10.1016/j.ymssp.2019.03.046.

Ali M. Seismic performance of coconut-fibre-reinforced-concrete columns with different reinforcement configurations of coconut-fibre ropes. Construction and Building Materials. 2014; 70 : 226-230. doi:10.1016/j.conbuildmat.2014.07.086.

Antonucci R, Balducci F, Bartera F, Castellano MG, Chaudat T. Shaking table tests on r.c. frame braced with fluid viscous dampers.

Balsamo A, Colombo A, Manfredi G, Negro P, Prota A. Seismic behavior of a full-scale RC frame repaired using CFRP laminates. *Engineering Structures*. 2005;27(5):769-780. doi:10.1016/j.engstruct.2005.01.002.

Bournas DA. Concurrent seismic and energy retrofitting of RC and masonry building envelopes using inorganic textile-based composites combined with insulation materials: A new concept. *Composites Part B: Engineering*. 2018;148:166-179. doi:10.1016/j.compositesb.2018.04.002.

Chalioris, C.E.; Karayannis, C.G.; Angeli, G.M.; Papadopoulos, N.A.; Favvata, M.J.; Providakis, C.P. Applications of Smart Piezoelectric Materials in a Wireless Admittance Monitoring System (WiAMS) to Structures-Tests in RC Elements. Case Stud. Constr. Mater. 2016, 5, 1-18, doi:10.1016/j.cscm.2016.03.003.

Chalioris CE, Kytinou VK, Voutetaki ME, Karayannis CG. Flexural Damage Diagnosis in Reinforced Concrete Beams Using a Wireless Admittance Monitoring System—Tests and Finite Element Analysis. Sensors 2021; 21(3). DOI: https://doi.org/10.3390/s21030679.

Chalioris C, Voutetaki M, Liolios A. Structural Health Monitoring of Seismically Vulnerable RC Frames under Lateral Cyclic Loading. Earthquakes and Structures 2020; 19(1): 29–44.

Chaudat T, Pilakoutas K, Papastergiou P, Ciupala MA. SHAKING TABLE TESTS ON REINFORCED CONCRETE RETROFITTED FRAME WITH FIBERGLASS REINFORCED PLASTIC (FRP). First European Conference on Earthquake Engineering and Seismology. September: 2006

Dalley S. Ancient Mesopotamian Gardens and the Identification of the Hanging Gardens of Babylon Resolved. Garden History 1993; 21(1): 1. DOI: https://doi.org/10.2307/1587050.

Del Vecchio C., Di Ludovico M., Balsamo A., Prota A., Manfredi G., Dolce M., Experimental investigation of exterior RC beam-column joints retrofitted with FRP systems, Journal of Composites for Construction, 2014, Volume 18, Issue 4, https://doi.org/10.1061/(ASCE)CC.1943-5614.0000459

Del Vecchio C., Di Ludovico M., Balsamo A., Prota A., Seismic Strengthening of RC Beam-Column Joints with FRP Systems Applicable from the Exterior of the Building, Special Publication, 2024a, Volume 360, p. 462-473, DOI: 10.14359/51740643

Del Vecchio C., Di Ludovico M., Balsamo A., Prota A., Minimally Invasive FRP Strengthening of External Beam–Column Joints, Journal of Composites for Construction, 2024b, Volume 28, Issue 4, https://doi.org/10.1061/JCCOF2.CCENG-4525

Di Michele F, Spacone E, Camata G, et al. Shaking table test and numerical analyses of a full scale three-leaf masonry wall. *Bull Earthquake Eng*. 2023;21(10):5041-5081. doi:10.1007/s10518-023-01705-y.

Fardis MN. Design provisions for masonry-infilled RC frames. Proceedings of 12th World Conference on Earthquake Engineering, Auckland, New Zeland: 2000.

Fiorentino G, Cengiz C, De Luca F, et al. SHAKING TABLE TESTS ON AN INTEGRAL ABUTMENT BRIDGE MODEL: PRELIMINARY RESULTS. In: *Proceedings of the 7th International Conference on Computational Methods in Structural Dynamics and Earthquake Engineering (COMPDYN 2015)*. Institute of Structural Analysis and Antiseismic Research School of Civil Engineering National Technical University of Athens (NTUA) Greece; 2019:3644-3655. doi:10.7712/120119.7176.19103.

Foster KP. The Hanging Gardens of Nineveh. Iraq 2004; 66: 207. DOI: https://doi.org/10.2307/4200575.

Gams M, Tomaževič M, Berset T. Seismic strengthening of brick masonry by composite coatings: an experimental study. Bulletin of Earthquake Engineering 2017; 15(10): 4269–4298.

Garcia R, Pilakoutas K, Hajirasouliha I, Guadagnini M, Kyriakides N, Ciupala MA. Seismic retrofitting of RC buildings using CFRP and post-tensioned metal straps: shake table tests. *Bull Earthquake Eng*. 2017;15(8):3321-3347. doi:10.1007/s10518-015-9800-8.

Gioffrè M, Cavalagli N, Gusella V, Pepi C. Confined vs. unreinforced masonry: Construction and shaking table tests of two-storey buildings. *Construction and Building Materials*. 2022;333:126961. doi:10.1016/j.conbuildmat.2022.126961.

Golias E, Zapris AG, Kytinou VK, Osman M, Koumtzis M, Siapera D, Chalioris CE, Karayannis CG. Application of X-Shaped CFRP Ropes for Structural Upgrading of Reinforced Concrete Beam–Column Joints under Cyclic Loading–Experimental Study. Fibers 2021; 9(7).

Guo R, Zhang H, Chen K, et al. Seismic Performance Analysis of Concrete Columns Reinforced with Prestressed Wire Ropes Embedded in Polyurethane Cement Composites. *Buildings*. 2024 ; 14 (4) : 993. doi:10.3390/buildings14040993.

Hanging Gardens of Babylon. Wikipedia 2022.

https://en.wikipedia.org/w/index.php?tle=Hanging_Gardens_of_Babylon&oldid=1114135823.

Helman D, Yungstein Y, Mulero G, Michael Y. High-Throughput Remote Sensing of Vertical Green Living Walls (VGWs) in Workplaces. Remote Sensing 2022; 14(14): 3485.

Hojdys Ł, Krajewski P, Kwiecien A, Rousakis T, Vanian V, Marcin T, Viskovic A, Ilki A, Gams M, Rakicevic Z, Zajac B, Bogdanovic A. Quick Repair of Damaged Infill Walls with Externally Bonded FRPU Composites: Shake Table Tests. Journal of Composites for Construction ASCE. Volume 27, Issue 1.February: 2023. https://doi.org/10.1061/(ASCE)CC.1943-5614.0001268

Hou S, Zhang H, Han X, Ou J. Damage monitoring of the RC frame shaking table test and comparison with FEM results. Procedia Engineering 2017; 210: 393–400.

Irga PJ, Torpy FR, Griffin D, Wilkinson SJ. Vertical Greening Systems: A Perspective on Existing Technologies and New Design Recommendation. *Sustainability*. 2023;15(7):6014. doi:10.3390/su15076014.

Karabini, M.; Rousakis, T.; Golias, E.; Karayannis, C. Seismic tests of full scale reinforced concrete T joints with light external continuous composite rope strengthening—Joint deterioration and failure assessment. Materials 2023, 16(7), 2718; https://doi.org/10.3390/ma16072718

Karabinis A., Rousakis T., Lappa M.; Laboratory of reinforced concrete and seismic design of structures. Technika chronika., Issue 4. Athens 2008, http://library.tee.gr/vufind/Record/tx2%2F12702.

Karantzikis M, Papanicolaou CG, Antonopoulos CP, Triantafillou TC. Experimental Investigation of Nonconventional Confinement for Concrete Using FRP. Journal of Composites for Construction 2005; 9(6): 480–487. DOI: https://doi.org/10.1061/(ASCE)1090-0268(2005)9:6(480).

Karayannis C, Golias E, Kalogeropoulos G, Influence of Carbon Fiber-Reinforced Ropes Applied as External Diagonal Reinforcement on the Shear Deformation of RC Joints, Fibers 2022, 10(3), 28; https://doi.org/10.3390/fib10030028

Karayannis C, Golias E, Full-scale experimental testing of RC beam-column joints strengthened using CFRP ropes as external reinforcement, Engineering Structures, Volume 250, 1 January 2022, 113305, https://doi.org/10.1016/j.engstruct.2021.113305

Karayannis CG, Voutetaki ME, Chalioris CE, Providakis CP, Angeli GM. Detection of flexural damage stages for RC beams using Piezoelectric sensors (PZT). Smart Structures and Systems, An International Journal 2015; 15(4): 997–1018.

Katsamakas AA, Vassiliou MF, Mouzakis C. Shake table testing and finite element modeling of a modular prefabricated concrete bridge-like specimen accounting for geometry imperfections and additional damping. Earthquake Engng Struct Dyn. 2024; 53: 3607–3629. https://doi.org/10.1002/eqe.4189

Koutas L, Triantafillou TC, Bousias SN. Analytical Modeling of Masonry-Infilled RC Frames Retrofitted with Textile-Reinforced Mortar. Journal of Composites for Construction 2015; 19(5): 04014082.

Kwiecień A, Gams M, Rousakis T, Viskovic A, Korelc J. Validation of a New Hyperviscoelastic Model for Deformable Polymers Used for Joints between RC Frames and Masonry Infills. Engineering Transactions 2017; 65(1): 113–121.

Kwiecień A. Shear bond of composites-to-brick applied with highly deformable, in relation to resin epoxy, interface materials. Materials and Structures 2014; 47(12): 2005–2020.

Kwiecień A, Zając B. Dynamic response of the cracked masonry building repaired with the flexible joint method – an innovative earthquake protection. In: Brennan MJ, editor. Proceedings of the 7th European Conference on Structural Dynamics, 7-9 July 2008, Southampton: University of Southampton. Institute of Sound & Vibration Research; 2008.

Kwiecień A, de Felice G, Oliveira DV, Zając B, Bellini A, De Santis S, et al. Repair of composite-tomasonry bond using flexible matrix. Materials and Structures 2016; 49(7): 2563–2580.

Manouchehri M, Santiago López J, Valiente López M. Sustainable Design of Vertical Greenery Systems: A Comprehensive Framework. *Sustainability*. 2024;16(8):3249. doi:10.3390/su16083249.

Marugg C. Vertical Forests: The Impact of Green Balconies on the Microclimate by Solar Shading, Evapotranspiration and Wind Flow Change: 2018.

Na, W.S; Baek, J., A Review of the Piezoelectric Electromechanical Impedance Based Structural Health Monitoring Technique for Engineering Structures, Sensors 2018, 18(5), 1307; doi:10.3390/s18051307.

Nakashima M, Nagae T, Enokida R, Kajiwara K. Experiences, accomplishments, lessons, and challenges of E-defense—Tests using world's largest shaking table. *Japan Architectural Review*. 2018;1(1):4-17. doi:10.1002/2475-8876.10020.

Ozden S, Akguzel U, Ozturan T. Seismic strengthening of infilled reinforced concrete frames with composite materials. ACI Structural Journal 2011; 108(4): 414–422.

Padanattil A, Karingamanna J, K.M M. Novel hybrid composites based on glass and sisal fiber for retrofitting of reinforced concrete structures. Construction and Building Materials 2017; 133: 146–153.

Papadopoulos, N.A.; Naoum, M.C.; Sapidis, G.M.; Chalioris, C.E. Cracking and Fiber Debonding Identification of Concrete Deep Beams Reinforced with C-FRP Ropes against Shear Using a Real-Time Monitoring System. Polymers 2023, 15, 473, doi:10.3390/polym15030473.

Providakis C, Tsistrakis S, Voutetaki M, Tsompanakis Y, Stavroulaki M, Agadakos J, Kampianakis E, Pentes G. A new damage identification approach based on impedance-type measurements and 2D error statistics. Structural Monitoring and Maintenance 2015; 2(4): 319–338.

Providakis C, Tsistrakis S, Voutetaki M, Tsompanakis J, Stavroulaki M, Agadakos J, Kampianakis E, Pentes G, Liarakos E. An Innovative Active Sensing Platform for Wireless Damage Monitoring of Concrete Structures. Current Smart Materials 2016; 1(1): 49–62.

Reade J. Alexander the Great and the Hanging Gardens of Babylon. Iraq 2000; 62: 195. DOI: https://doi.org/10.2307/4200490.

Reade J. Alexander the Great and the Hanging Gardens of Babylon. Iraq 2000; 62: 195. DOI:https://doi.org/10.2307/4200490.

Rouka D, Kaloudaki A, Rousakis T, Fanaradelli T, Anagnostou E, Kwiecień A, et al. Response of RC buildings with Low-strength Infill Walls Retrofitted with FRP sheets with Highly Deformable Polymer-Effects of Infill Wall Strength. 25th International Conference on Composites/Nano Engineering, Rome 2017.

Rousakis TC, Tourtouras IS. RC columns of square section – Passive and active confinement with composite ropes. Composites Part B: Engineering 2014; 58: 573–581.

Rousakis TC. Reusable and recyclable nonbonded composite tapes and ropes for concrete columns confinement. Composites Part B: Engineering 2016; 103: 15–22.

Rousakis T, Ilki A, Kwiecien A, Viskovic A, Gams M, Triller P, Ghiassi B, Benedetti A, Rakicevic Z,Colla C, Halici OF, Zając B, Hojdys Ł, Krajewski P, Rizzo F, Vanian V, Sapalidis A, Papadouli E, Bogdanovic A. Deformable Polyurethane Joints and Fibre Grids for Resilient Seismic Performance of Reinforced Concrete Frames with Orthoblock Brick Infills. Polymers 2020; 12(12). DOI: https://doi.org/10.3390/polym12122869.

Rousakis T, Anagnostou E, Fanaradelli T. Advanced Composite Retrofit of RC Columns and Frames with Prior Damages—Pseudodynamic Finite Element Analyses and Design Approaches. Fibers 2021a; 9(9).

Rousakis T, Vanian V, Fanaradelli T, Anagnostou E. 3D FEA of Infilled RC Framed Structures Protected by Seismic Joints and FRP Jackets. Applied Sciences 2021b; 11(14).

Rousakis TC, Panagiotakis GD, Archontaki EE, Kostopoulos AK. Prismatic RC columns externally confined with FRP sheets and pre-tensioned basalt fiber ropes under cyclic axial load. Composites Part B: Engineering 2019; 163: 96–106. DOI: https://doi.org/10.1016/j.compositesb.2018.11.024.

Rousakis T, Tourtouras I. RC columns of square section – Passive and active confinement with composite ropes. *Composites Part B: Engineering*. 2014;58:573-581. doi:10.1016/j.compositesb.2013.11.011.

Rousakis T, Macha M. External Confinement with Basalt Fiber Ropes in Existing Reinforced Concrete Structures. *ce papers*. 2023;6(5):277-285. doi:10.1002/cepa.2109.

Sam-Daliri, O.; Faller, L.M.; Farahani M.; Roshanghias, A.; Araee, A.; Baniassadi, M.; Oberlercher, H.; Zangl, H., Impedance analysis for condition monitoring of single lap CNT-epoxy adhesive joint. International Journal of Adhesion and Adhesives, 88, 59-65, doi:10.1016/j.ijadhadh.2018.11.003.

Sam-Daliri, O.; Faller, L.M.; Farahani M.; Zangl, H., Structural health monitoring of adhesive joints under pure mode I loading using the electrical impedance measurement. Engineering Fracture Mechanics, 245, 107585, doi:10.1016/j.engfracmech.2021.107585.

Sharma R, Hsiao FP, Liu KY, Pon CE. Shaking table test of a half-scale three-story non-ductile RC building subjected to near-fault ground motions: Experimental and numerical modeling. *Structures*. 2022;45:721-747. doi:10.1016/j.istruc.2022.09.041.

Talakokula V, Bhalla S, Gupta A. Corrosion assessment of reinforced concrete structures based on equivalent structural parameters using electro-mechanical impedance technique. Journal of Intelligent Material Systems and Structures 2014; 25(4): 484–500. DOI: https://doi.org/10.1177/1045389X13498317.

Talakokula V, Bhalla S. Reinforcement corrosion assessment capability of surface bonded and embedded piezo sensors for reinforced concrete structures. Journal of Intelligent Material Systems and Structures 2015; 26(17): 2304–2313. DOI: https://doi.org/10.1177/1045389X14554133.

Tedeschi C, Kwiecień A, Valluzzi MR, Zając B, Garbin E, Binda L. Effect of thermal ageing and salt decay on bond between FRP and masonry. Materials and Structures 2014; 47(12): 2051–2065.

Triantafillou TC, Papanicolaou CG, Zissimopoulos P, Laourdekis T. Concrete confinement with textile- reinforced mortar jackets. ACI Structural Journal 2006; 103(1): 28.

Urban Forestry. Stefano Boeri Architetti. https://www.stefanoboeriarchitetti.net/en/urban-forestry/.

Voutetaki ME, Papadopoulos NA, Angeli GM, Providakis CP. Investigation of a new experimental method for damage assessment of RC beams failing in shear using piezoelectric transducers. Engineering

Structures 2016; 114: 226–240. DOI: https://doi.org/10.1016/j.engstruct.2016.02.014.

Voutetaki ME, Naoum MC, Papadopoulos NA, Chalioris CE. Cracking Diagnosis in Fiber- Reinforced Concrete with Synthetic Fibers Using Piezoelectric Transducers. Fibers 2022; 10(1).

Wang X, Gard W, van de Kuilen JW. Vertical Forest Engineering: Applications of Vertical Forests with Self-Growing Connections in High-Rise Buildings. In van de Kuilen JW, Gard W, editors, ISCHP 2019 - 7th International Scientific Conference on Hardwood Processing. Delft: Delft University of Technology. 2019. p. 184-197.

Yuksel E, Ilki A, Erol G, Demir C, Karadogan HF. Seismic retrofit of infilled reinforced concrete frames with cfrp composites. In: Wasti ST, Ozcebe G, editors. Advances in Earthquake Engineering for Urban Risk Reduction, Dordrecht: Springer Netherlands; 2006.